Clays and Clay Minerals, Vol. 42, No. 3, 337–355, 1994.

MOLECULAR STRUCTURE AND BINDING SITES OF COBALT(II) SURFACE COMPLEXES ON KAOLINITE FROM X-RAY ABSORPTION SPECTROSCOPY

PEGGY A. O'DAY,[1] GEORGE A. PARKS, AND GORDON E. BROWN JR.

Surface and Aqueous Geochemistry Group, School of Earth Sciences,
Stanford University, Stanford, California 94305 USA

Abstract—X-ray absorption spectroscopy (XAS) was used to determine the local molecular environment of Co(II) surface complexes sorbed on three different kaolinites at ambient temperature and pressure in contact with an aqueous solution. Interatomic distances and types and numbers of backscattering atoms have been derived from analysis of the extended X-ray absorption fine structure (EXAFS). These data show that, at the lowest amounts of Co uptake on kaolinite (0.20–0.32 μmol m^{-2}), Co is surrounded by $\approx$6 O atoms at 2.04–2.08 Å and a small number of Al or Si atoms (N = 0.6–1.5) at two distinct distances, 2.67–2.72 Å and 3.38–3.43 Å. These results indicate that Co bonds to the kaolinite surface as octahedrally coordinated, bidentate inner-sphere mononuclear complexes at low surface coverages, confirming indirect evidence from solution studies that a fraction of sorbed Co forms strongly bound complexes on kaolinite. In addition to inner-sphere complexes identified by EXAFS spectroscopy, solution studies provide evidence for the presence of weakly bound, outer-sphere Co complexes that cannot be detected directly by EXAFS. One orientation for inner-sphere complexes indicated by XAS is bidentate bonding of Co to oxygen atoms at two Al-O-Si edge sites or an Al-O-Si and Al-OH (inner hydroxyl) edge site, i.e., corner-sharing between Co octahedra and Al and Si polyhedra. At slightly higher surface sorption densities (0.51–0.57 μmol m^{-2}), the presence of a small number of second-neighbor Co atoms (average $N_{Co} < 1$) at 3.10–3.13 Å indicates the formation of oxy- or hydroxy-bridged, multinuclear surface complexes in addition to mononuclear complexes. At these surface coverages, Co-Co and Co-Al/Si distances derived from EXAFS are consistent with edge-sharing between Co and Al octahedra on either edges or (001) faces of the aluminol sheet in kaolinite. Multinuclear complexes form on kaolinite at low surface sorption densities equivalent to <5% coverage by a monolayer of oxygen-ligated Co octahedra over the N_2-BET surface area. These spectroscopic results have several implications for macroscopic modeling of metal ion uptake on kaolinite: 1) Primary binding sites on the kaolinite surface at low uptake are edge, non-bridging Al-OH inner hydroxyl sites and edge Al-O-Si bridging oxygen sites, not Si-OH sites typically assumed in sorption models; 2) specific adsorption of Co is via bidentate, inner-sphere complexation; and 3) at slightly higher uptake but still a small fraction of monolayer coverage, formation of Co multinuclear complexes, primarily edge-sharing with Al-OH octahedra, begins to dominate sorption.

Key Words—Cobalt, EXAFS, Kaolinite, Sorption, Surface complex.

INTRODUCTION

In surface waters and groundwater, chemical bonding of solutes to clay mineral surfaces to form surface complexes is an important regulator of the migration and concentration of toxic and radioactive species. Over many years of investigation, attention has been focused on the description and understanding of chemical interactions that occur between sorbed species and their mineral substrates (see, e.g., recent books by Dzombak and Morel, 1990; Stumm, 1992; and volumes edited by Davis and Hayes, 1986; Stumm, 1987; Hochella and White, 1990). Recent work has demonstrated the utility of spectroscopy in providing insight into microscopic properties of aqueous species sorbed at mineral surfaces and, in some cases, has given direct molecular confirmation of hypotheses inferred from macroscopic measurements (Motschi, 1987; Hayes *et al.*, 1987; Brown and Parks, 1989; Brown *et al.*, 1989; Bancroft and Hyland, 1990; Brown, 1990). Spectroscopic probes can provide structural and chemical information about how surface complexes bind to substrates and, ideally, they should reveal atomic and molecular characteristics consistent with and complementary to macroscopic chemical behavior.

In this study, X-ray absorption spectroscopy (XAS) was used to investigate directly the local molecular coordination of low surface coverages of Co sorbed to kaolinite at ambient temperature and pressure over an order-of-magnitude range in sorption density. Spectroscopic data were collected *in situ*, i.e., with an aqueous solution (Co + $NaNO_3$) present and in contact with the kaolinite surface. Extended X-ray absorption fine structure (EXAFS) spectra, obtained using synchrotron X-rays and fluorescence-yield detection, were analyzed quantitatively for low levels of sorbed Co (0.20–2.6 μmol m^{-2}). Cobalt(II) was chosen as the absorber atom because it is a toxic and, in some contexts, radioactive contaminant, and its chemical behavior is represen-

[1] Present address: Department of Geology and Geophysics, University of California, Berkeley, California 94720.

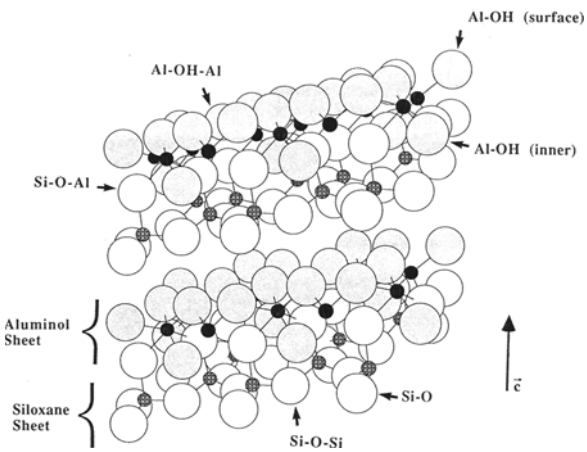

Figure 1. Kaolinite crystal structure showing the aluminol and siloxane sheets forming 1:1 layers, and surface oxygen atoms exposed on faces that may act as reactive surface sorption sites. Atoms: Al = solid; Si = hatched; O = open; OH = shaded.

tative of other divalent transition metal ions common in natural systems and used in industrial processes. Kaolinite, a relatively common and simple clay mineral obtainable in near-chemically pure form, serves as a well-characterized substrate that can be used to deduce sites of Co binding on the mineral surface. Analysis of EXAFS spectra gives average interatomic distances (accuracy of ±0.02 Å), and types and numbers of nearest-neighbor atoms to distances of about 4 Å around a central Co atom. In this paper, we discuss variations in the X-ray absorption spectra that reflect changes in the geometry and binding sites of mononuclear and multinuclear Co surface complexes with increasing uptake on different kaolinites, and we relate these observations to macroscopic sorption behavior. The structures of multinuclear Co surface complexes and surface precipitates observed at high sorption densities using EXAFS analysis are discussed elsewhere (O'Day *et al.*, 1994a).

Analysis of the EXAFS spectrum is particularly useful in the study of sorbed atoms because 1) it is specific to the element of interest and usable at ambient conditions for all elements of atomic number (Z) greater than ≈20; 2) it is a non-vacuum technique applicable to solids, liquids, and suspensions, and it is very sensitive to low concentrations of the absorbing atom when fluorescence or electron yield is measured; 3) interatomic distances between a central absorber, first-neighbor atoms, and, in favorable cases, distant neighbor atoms (≈3–6 Å) can be determined to an accuracy of ±0.02 Å or better, even in disordered systems; and 4) different atomic backscatterers can be readily distinguished if they differ in Z by greater than about ±3 (Brown *et al.*, 1988). Unfortunately, XAS has several significant limitations in this study, some inherent in the technique and others stemming from the use of Co as the absorber atom and relatively light atoms from kaolinite, O, Al, and Si, as backscatterers. First, XAS samples average atomic structure and thus, the spectra represent a sum of all Co bonding environments, including all types and numbers of near-neighbor atomic backscatterers around Co and all positional and vibrational disorder. Therefore, numerical information from EXAFS analysis must be combined with structural models of the local chemical environment to deduce specific sorption sites. Second, Al and Si atoms cannot be distinguished from each other as backscatterers in kaolinite because they differ by Z = 1 and their backscattering character is too similar to produce distinct phase-shift and amplitude functions. Last, although fluorescence XAS is very sensitive to low absorber concentrations, it is not sensitive to low concentrations of backscattering atoms or to backscatterers of low Z. In spite of these limitations, EXAFS analysis is one of the few methods for obtaining quantitative information about the average structure of *in situ* surface complexes and their bonding geometry on surfaces.

SORPTION AND SORPTION SITES ON KAOLINITE

Kaolinite is 1:1 dioctahedral clay with 7 Å spacing that has no structural charge in its pure stoichiometric form (Grim, 1968; Giese, 1988). Sorption of aqueous species and development of surface charge are controlled mainly by amphoteric reactions at oxygen sites on aluminol and siloxane surfaces that are conceptually similar to surface reactions on oxide minerals (Sposito, 1984; Figure 1). Natural kaolinites do, however, have a small cation-exchange capacity, generally <0.02 mol charge kg^{-1} in chemically pure kaolinites (Talibudeen, 1981; Parfitt, 1978; Sposito, 1984, 1989) and thus, the surface properties of kaolinite share characteristics with both oxides and smectites. Weak, cation exchange-type sorption observed in macroscopic studies of kaolinite is generally attributed to two factors: either isomorphic substitution of Al^{3+} for Si^{4+} in the tetrahedral sheet giving rise to a negative structural charge or contamination by small amounts of 2:1 phyllosilicate minerals (Schofield and Samson, 1954; Bolland *et al.*, 1976, 1980; Ferris and Jepson, 1975; van Olphen, 1977; Sposito, 1984; Schindler *et al.*, 1987; Wieland and Stumm, 1992). Several experimental studies suggest that both factors may contribute to ion exchange (Jepson and Rowse, 1975; Lee *et al.*, 1975; Lim *et al.*, 1980; Talibudeen and Goulding, 1983). There is disagreement, however, over whether apparent exchange properties arise from isomorphic substitution and/or contamination only, or whether some exchange-type behavior is pH-dependent and related to the sorption of charged species (Ferris and Jepson, 1975; Bolland *et al.*, 1976; van Olphen, 1977; Lim *et al.*, 1980).

Studies of divalent metal cation (Me^{2+}) uptake on kaolinite show that fractional uptake from solution is

https://doi.org/10.1346/CCMN.1994.0420312 Published online by Cambridge University Press

low at low pH, rises rapidly in a narrow pH range, and can exceed 95% below the pH of precipitation of a stable hydroxide (Figure 2). Uptake is reduced by order-of-magnitude increases in the concentration of the supporting electrolyte below pH ≈ 7–8, but uptake is insensitive to change in electrolyte concentration above this pH range (Figure 2a) (Schindler *et al.*, 1987; Cowan *et al.*, 1992; O'Day, 1992; Zachara *et al.*, 1994). Based on solution uptake experiments and potentiometric titrations, uptake of cations, anions, and/or protons from solution onto kaolinite as a function of pH is generally modeled assuming two classes of sites: 1) ion exchange or nonspecific adsorption sites that exchange background electrolyte cations with weakly bound, hydrated adions ("outer-sphere" complexes) and 2) specific adsorption at amphoteric surface hydroxyl sites (e.g., Al-OH, Si-OH) in which surface sites hydrolyze and adions bond directly to surface oxygens such that they are not easily displaced by electrolyte ions ("inner-sphere" complexes) (Farrah *et al.*, 1980; Riese, 1982; Sposito, 1984; Schindler *et al.*, 1987; Zachara *et al.*, 1988; Carroll-Webb and Walther, 1988; Cowan *et al.*, 1992; Singh and Mattigod, 1992; Wieland and Stumm, 1992; Xie and Walther, 1992; Zachara *et al.*, 1994). In these previous macroscopic studies, however, different models of ion uptake have reproduced experimental data equally well and do not supply a unique solution. These models have differed significantly in the number and types of reactions included, in the surface sorption sites chosen to bind cations, in whether complexes bind as inner-sphere or outer-sphere, and in the values of the stability constants used to describe sorption reactions.

Surface sites on kaolinite that may take part in sorption reactions can be examined by considering the ideal kaolinite structure and the way in which O atoms and OH groups are coordinated to Al and Si atoms (Sposito, 1984; Giese, 1988). In kaolinite, there are O atoms in six structurally unique sites (Figure 1): 1) non-bridging (single-bonded) Al-OH exposed at edges of the aluminol sheet ("surface OH"); 2) non-bridging Al-OH at edges in between the aluminol and siloxane sheets ("inner OH"); 3) non-bridging Si-O exposed at edges of the siloxane sheet; 4) bridging Al-O-Si between the aluminol and siloxane sheet exposed at edges; 5) bridging Al-OH-Al exposed on (001) faces of the aluminol sheet; and 6) bridging Si-O-Si exposed on (001) faces of the siloxane sheet. On edges, non-bridging Al-OH (inner and surface) and Si-O have long been regarded as the most reactive surface sites that can sorb protons and ions (Schofield and Samson, 1954; Follet, 1965; Fordham, 1973; Parfitt, 1978; Sposito, 1984), but the Al-O-Si site is usually not considered in sorption reactions. Bridging Si-O-Si sites on (001) faces are considered unreactive (Sposito, 1984; Davis and Kent, 1990), but there is disagreement over whether or not bridging Al-OH-Al sites on (001) faces react significantly (Sposito, 1984; Carroll-Webb and Walther, 1988; Wieland and Stumm, 1992). Because kaolinite is a dioctahedral clay, stoichiometric Al vacancies in the aluminol sheet may give rise to localized negative charge, and it is not known how vacancies affect the reactivity of oxygen atoms exposed at particle surfaces. Finally, the ditrigonal cavity on the siloxane surface functions as a soft Lewis base when permanent structural charge exists in the siloxane or aluminol sheets, but its reactivity in uncharged kaolinite particles is considered low

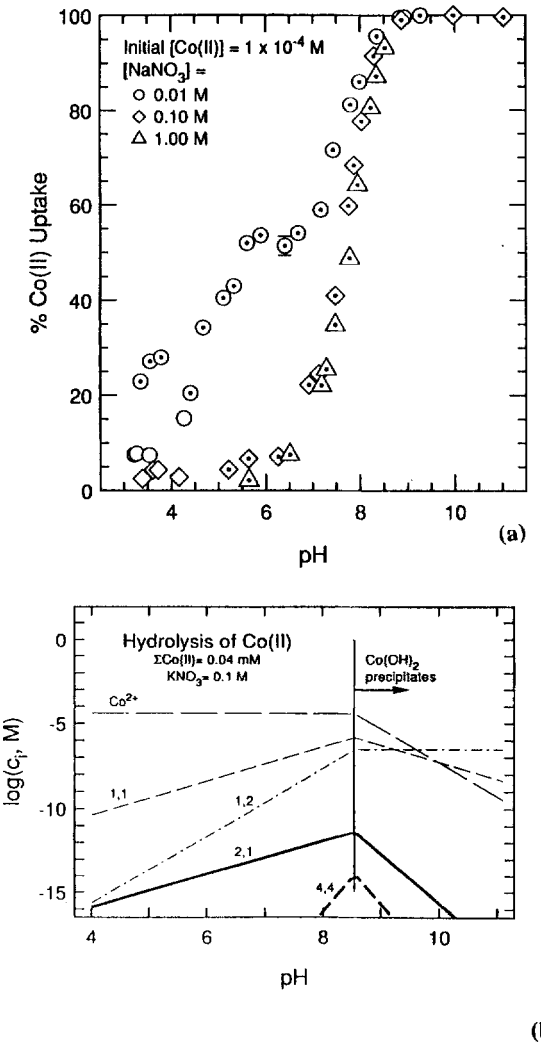

Figure 2. a) Cobalt uptake (% Co removed from solution) on <2 μm DB kaolinite as a function of pH at three different concentrations of background electrolyte ([$NaNO_3$] = 0.01, 0.1, 1.0 M) and total [Co(II)] = 1 × 10^{-4} M. Error bar is ±4% uptake estimated from counting statistics for radioactive decay. Open symbols = pre-equilibration with pH 3.2 $NaNO_3$ solutions; dotted symbols = pre-equilibration with pH 6 $NaNO_3$ solutions (see O'Day, 1992, for details of uptake experiments). b) Distribution of Co(II) species in aqueous solution as a function of pH at total Co concentration of 4 × 10^{-5} M, equivalent to 60% Co uptake from solution.

https://doi.org/10.1346/CCMN.1994.0420312 Published online by Cambridge University Press

(Sposito, 1984). This view is supported by recent *ab initio* quantum chemical calculations on the bulk kaolinite structure that suggest only a small amount of localized negative charge density in the ditrigonal cavity from oxygen lone-pair electrons (Hess and Saunders, personal communication).

SPECTROSCOPIC STUDIES OF SORBED METAL IONS

X-ray photoelectron spectroscopy (XPS) and electron spin resonance (ESR) studies of transition metal ions sorbed to oxides and clays provide evidence that the adion complex is similar to the aqueous hexaaquo Me(II or III) ion at low pH and that the electronic structure of the adion changes with increasing pH. In a series of investigations, metal ions (Co(II), Ni(II), Cr(III), Fe(III)) sorbed to clays and oxides (kaolinite, illite, chlorite, goethite) as a function of increasing pH were studied by XPS (Koppelman and Dillard, 1975, 1977; Koppelman *et al.,* 1980; Dillard and Koppelman, 1982; Schenk *et al.,* 1983). Based on changes in binding energies and peak intensities, these studies concluded that the bonding environment of the metal cation becomes "more ionic" with increasing pH. They suggested a change from a dominantly aquo surface complex to a more hydroxide-like complex but one that is not identical to the solid hydroxide phase most likely to precipitate. Other XPS studies of Co(II) complexes on γ-Al_2O_3 suggest a correlation between hydrolysis, adsorption, and the formation of aquo-type complexes at low pH and possible formation of a surface precipitate at high pH (Tewari *et al.,* 1972; Tewari and Lee, 1975; Tewari and McIntyre, 1975). Cobalt and Ni sorption on hectorite and montmorillonite studied by XPS (Davison *et al.,* 1991) supported previous results indicating the formation of a hydroxide-like species at high pH and no change in the binding energies of the sorbed species after successive washings, implying strong bonding of the cation to the surface. Electron spin resonance (ESR) has been used to probe surface complexes of Cu^{2+} and Mn^{2+} on kaolinite (McBride, 1976, 1978) and other oxides *in situ* (McBride *et al.,* 1984; Motschi, 1984; Bleam and McBride, 1985). From ESR data, McBride (1976) concluded that sorption sites are distributed evenly over basal planes and edges on kaolinite and that Cu^{2+} exists as planar $Cu(H_2O)_4^{2+}$ complexes alligned parallel to planar kaolinite surfaces. Formation of surface multinuclear species has also been proposed based on ESR results (Bleam and McBride, 1985). Motschi (1987), however, argues that the distances between atoms in these "clusters" cannot be quantified with ESR and may extend for 10–20 Å; thus, the adatoms are not actually bonded in a cluster. The results of XPS and ESR studies, while not providing unique molecular descriptions of sorbed cations on kaolinite and oxide surfaces, provide evidence for the formation of strongly bound complexes and changes in the bonding of the adion with increasing pH.

More direct information about the structure of surface complexes comes from *in situ* EXAFS studies of metal cations sorbed to oxide and clay minerals. Studies of Co(II) complexes on oxides (γ-Al_2O_3, TiO_2, and SiO_2) indicate inner-sphere, multinuclear complex formation that may be influenced by the structure of the substrate (Chisholm-Brause *et al.,* 1990b; Chisholm-Brause, 1991; O'Day *et al.,* 1991). Inner-sphere, multinuclear complex formation is proposed for Pb(II) complexes on γ-Al_2O_3 (Chisholm-Brause *et al.,* 1990a) and goethite (Roe *et al.,* 1991), Pb(II) on hydrous Mn-oxide (Manceau *et al.,* 1992), and Cr(III) on Mn- and Fe-oxide (Charlet and Manceau, 1992; Manceau and Charlet, 1992). Inner-sphere, mononuclear bidentate complexes are proposed for Pb(II) and UO_2^{2+} on hydrous Fe-oxide (Manceau *et al.,* 1992). An EXAFS study of U(VI) sorption on montmorillonite and silica suggested that the formation of monomeric or multinuclear species depends on pH and U concentration (Dent *et al.,* 1992). In general, results from EXAFS studies show that cations bond to mineral surfaces primarily as bidentate, inner-sphere complexes. These studies also indicate formation of multinuclear complexes at relatively low surface loadings and an increase in the number of second-neighbor metal backscatterers as surface loading increases.

EXPERIMENTAL METHODS

Sample preparation

Three different kaolinites from south-central Georgia were used in this study: Dry Branch (DB) (May *et al.,* 1986), Purvis School Mine (PS), and M & M Mine (MM) (provided and characterized by H.M. May, U.S. Geological Survey, Boulder, Colorado). Bulk kaolinite was prepared (by USGS) as follows (after Jackson, 1975). Samples were treated with pH 5 Na-acetate solution (1 M) to disaggregate them and to replace other cations with Na, then with 30% H_2O_2 (3 additions) to oxidize and remove organic material. A citrate-bicarbonate-dithionite solution was used to remove iron oxides; final washings were done with NaCl (1 M) and then methanol-water solutions. Washed and dried samples were resuspended in distilled water and centrifuged to fractionate particle sizes. After separation, fractionated samples were air-dried and stored in a dessicator over drierite.

Unoriented samples of the <2 μm fraction were characterized by X-ray diffraction (XRD) using a Siemens D-500 diffractometer and Cu$K\alpha$ radiation (USGS). All XRD peaks were attributed to kaolinite and indicate well-crystallized samples, with the sharpness of small hkl reflections increasing in the order PS $<$ DB $<$ MM. A chemical analysis of each size fraction was obtained by X-ray fluorescence (XRF) (ARL 8400

Table 1. Chemical analysis by XRF (±1 wt. %) and surface area (N_2 BET method) of kaolinites used in XAS experiments.

	Dry Branch (<2 μm)	Purvis School (<2 μm)	M&M (<2 μm)
Wt. % oxides[1]			
SiO_2	45.0	44.6	44.1
AL_2O_3	39.3	38.3	38.5
Fe_2O_3	0.15	0.93	0.19
TiO_2	1.75	1.97	3.22
MgO (0.12%)	—	0.12	—
K_2O (0.02%)	—	0.03	—
P_2O_5 (0.05%)	0.06	0.07	0.15
LOI[2] (925°C)	13.9	14.0	13.7
Surface area[3] ($m^2\ g^{-1}$)	10.8	21.5	13.3

[1] Blanks (—) indicate concentrations below XRF detection limit (given in parentheses). CaO (0.02%), Na_2O (0.15%), and MnO (0.02%) below detection in all samples.
[2] Loss on ignition.
[3] Measured by N_2 BET.

spectrometer) on fused, polished beads of lithium metaborate and kaolinite (10:1 mixture) using standards selected for use with clay minerals and a normative program for kaolinite (estimated error is ±1 wt. %). Results of XRF analysis (Table 1) indicate a high degree of chemical purity. Surface areas (Table 1) were determined by a dynamic BET technique using N_2 adsorption (Micromeritics Flowsorb II 2300). Sample characterization by scanning and transmission electron microscopy and energy dispersive X-ray spectrometry (EDS) shows that small particles (0.05–0.2 μm in diameter) of TiO_2 (probably anatase) are the primary impurity (O'Day, 1992). In addition, electron microscopy revealed a few non-kaolinite particles, probably smectite by their composition from EDS, in the PS kaolinite sample.

Sorption samples for XAS were prepared by equilibration of individual batches of kaolinite (<2 μm fraction) with N_2-sparged aqueous $Co(NO_3)_2$ + $NaNO_3$ + NaOH solutions. Equilibration, sample handling, and pH-measurements were conducted in a N_2 atmosphere at ambient conditions (T = 22° ± 3°C). Table 2 summarizes initial and final solution concentrations ($Co(II)_{init}$ and $Co(II)_{final}$), final pH, and surface sorption density (Γ) for samples calculated according to:

$$\Gamma(\text{mol m}^{-2}) = \frac{[Co(II)_{init}](\text{mol liter}^{-1}) \times \%\ \text{uptake}}{\text{surface area}_{BET}(\text{m}^2\text{g}^{-1}) \times \text{solid conc.(g liter}^{-1})} \quad (1)$$

This definition of sorption density assumes that sorbed Co is distributed over the surface area as measured by BET gas adsorption. After initial equilibration (4–6 h) of kaolinite with $NaNO_3$ solutions, aqueous $Co(NO_3)_2$ spiked with carrier-free, radioactive Co^{57} (half-life = 270 days) obtained from E.I. du Pont de Nemours & Co. was added at the concentrations shown in Table 2. Solids were equilibrated with Co solutions at pH ≈ 6 for 6–12 h while mixing by rotation. Base (0.1 M NaOH) was then added to raise pH and sorb Co to the surface. Base was added dropwise while stirring the suspension to avoid local oversaturation with respect to solid hydroxide phases. After base addition and mixing by rotation for 24–36 h, pH was measured and a small aliquot (0.3–0.5 ml) of supernatant solution was removed and filtered (0.45 μm nylon membrane filter). For each different initial Co concentration, a blank Co solution was prepared in exactly the same manner as the sorption samples but with no solid present and no adjustment of pH with base. Cobalt activity from gamma radiation was measured in filtered, weighed supernatant solutions and in blank solutions with a Tracor Northern (TN-1750) Multichannel Analyzer. Uptake was calculated from the difference in counts between sample and blank by:

$$\%\ \text{uptake} = 100 \times \left[1 - \frac{\text{sample cts}(s^{-1}g^{-1}) - \text{bkgrd. cts}(s^{-1}g^{-1})}{\text{blank cts}(s^{-1}g^{-1}) - \text{bkgrd. cts}(s^{-1}g^{-1})}\right] \quad (2)$$

where "bkgrd. cts" are the measured background counts for an empty vial. In all experiments, initial and final solution concentrations were below thermodynamic

Table 2. Experimental solution conditions for Co/kaolinite sorption samples studied by XAS showing initial and final Co concentrations in solution ($[Co(II)_{init}]$ and $[Co(II)_{final}]$), final pH after sample equilibration ($pH_{(final)}$), and percent Co removed from solution.

Γ (10^{-6} mol m^{-2})	$[Co(II)_{init}]$ (10^{-3} mol liter^{-1})	$[Co(II)_{final}]$ (10^{-4} mol liter^{-1})	$pH_{(final)}$	% CO uptake
	Dry Branch kaolinite			
2.6	2.90	1.06	8.24	96.4
1.2	1.40	1.50	7.86	89.2
0.51	0.67	1.20	7.62	82.2
0.26	0.35	0.72	7.52	79.6
0.26, desorbed[1]	2.00	17.19	5.25	14.0
	Purvis School kaolinite			
1.2	2.70	2.59	7.88	90.4
0.57	1.40	1.83	7.74	86.9
0.28	0.68	0.78	7.77	88.6
0.21[2]	0.45	0.04	8.04	99.0
	M&M kaolinite			
0.32	0.56	1.37	7.63	75.5
0.30	0.42	0.18	8.08	95.6
0.20	0.28	0.27	7.85	90.1

Solid/liquid = 100 g/liter^{-1}
Background electrolyte = 0.10 M $NaNO_3$
Equilibration time = 24–36 h

Surface sorption density (Γ) is defined by Eq. 1.
[1] Co(II) desorbed to 14% uptake after equilibration for 24 h at 90% uptake.
[2] Background electrolyte = 0.01 M $NaNO_3$.

https://doi.org/10.1346/CCMN.1994.0420312 Published online by Cambridge University Press

solubilities reported for all solid $Co(OH)_2$ phases (Gayer and Garrett, 1950; Feitknecht and Schindler, 1963; Baes and Mesmer, 1976). For XAS measurements, sample slurries were centrifuged at 11,000 to 13,000 rpm for 35–45 min. Under N_2, excess supernatant solution was removed and samples were loaded as wet pastes into teflon sample holders and sealed with mylar windows. Spectra were also collected for 12 mM $Co(NO_3)_2$ aqueous solution, acidified to avoid hydrolysis, in a teflon/mylar sample holder.

An experimental spectrum of aged, synthetic $Co(OH)_2$(s) (dried pink form) was used as a reference for the unknown sorption samples. Identity and crystallinity of $Co(OH)_2$(s) were confirmed by X-ray powder diffraction. For XAS data collection, the solid was crushed with an agate mortar and pestle, and diluted with enough inert boron nitride to produce about 30% transmission of the incoming beam at the energy of the Co K-absorption edge. The mixture was loaded into an aluminum sample holder with mylar windows and transmission spectra were collected at ambient temperature and pressure.

XAS data collection

X-ray absorption spectra were collected at ambient temperature and pressure on wiggler magnet beamlines IV-1, IV-2, and IV-3 at the Stanford Synchrotron Radiation Laboratory (SSRL), Stanford, California, and on bending magnet beamline X11-A at the National Synchrotron Light Source (NSLS), Brookhaven National Laboratory, New York. Beam current at SSRL varied from 20 to 90 mA at 3 GeV and a wiggler field of 18 kG. At NSLS, beam current was 100 to 210 mA at 2.5 GeV. Either Si(111) or Si(220) monochromator crystals were used with an unfocused beam. Higher-order harmonic rejection was achieved by detuning the monochromator such that incoming beam flux was reduced by 30–50%. Beam energy was calibrated by assigning the first inflection on the absorption edge of metallic Co foil to an energy of 7709.3 eV. Fluorescence spectra for wet sorption samples were collected using a Stern-Heald-type detector (Lytle *et al.*, 1984) with Soller slits and an Fe filter to reduce background scattering and fluorescence. Fluorescence spectra for several low concentration samples were collected using a 13-element Ge array detector with a Be window. Transmission spectra were collected for the $Co(OH)_2$(s) model compound using gas-filled ion chambers.[2] Multiple scans (3–16 depending on Co concentration) were collected and averaged for each sample to improve signal-to-noise ratio. For fluorescence spectra, samples were oriented at a 45° angle with respect to the incoming beam. Because of the layered structure of kaolinite and the plane-polarized nature of synchrotron radiation, it is possible to have an angular dependence to X-ray absorption when structural elements of the sample are either coincident with, or perpendicular to, the polarization vector of the incoming beam (Heald and Stern, 1977; Hahn and Hodgson, 1983; Manceau *et al.*, 1988; Waychunas and Brown, 1990). To assess whether or not polarized absorption occurred in the kaolinite samples, a series of spectra were collected on one sorption sample over a range of angles with respect to the incoming beam (0° to 90°). At all orientations, the XAS spectra were identical and indicated no variations in absorption due to polarization.

XAS data reduction

Atomic information is derived from EXAFS spectra by defining a function, χ, in terms of parameters that relate the observed phase and amplitude of EXAFS oscillations to the distance, type, and number of backscatterer atoms around the central absorbing atom (see, e.g., reviews by Winick and Doniach, 1980; Teo and Joy, 1981; Teo, 1986; Koningsberger and Prins, 1988). The frequency of EXAFS oscillations is determined by the absorber-backscatterer distance (R) (i.e., longer R corresponds to higher frequency, shorter wavelength oscillations) and the amplitude is directly proportional to the number of backscatterers (N) at that distance. This can be expressed for a set of backscatterer atoms (N) at a particular distance (R) by

$$\chi(k) = \sum_R NS_0^2 \frac{|f_R(\pi, k)|}{kR^2} \cdot \sin(2kR + 2\delta^c + \Phi) e^{-2\sigma^2 k^2} e^{-2R/\lambda} \quad (3)$$

where $|f_R(\pi, k)|$ is the backscattering amplitude of the scatterer, δ^c and Φ are phase shifts for the absorber and backscatterer, respectively, S_0^2 is a many-body amplitude reduction factor, σ^2 is a Debye-Waller factor, λ is the mean free path of the electron, and k is the photoelectron wave vector, related to the kinetic energy of the photoelectron (E) by

$$k = \left[\frac{2m}{\hbar^2}(E - E_0)\right]^{1/2} \quad (4)$$

where E_0 is the threshold energy of the photoelectron at $k = 0$, $\hbar$ is Planck's constant/2π, and m is the mass of the electron. Numerical results are extracted from the EXAFS by known R and N for the same (or similar) absorber-backscatterer pair to an unknown spectrum.

The EXAFS spectra were analyzed using a curved-wave formalism (reviewed by Stern, 1988) and a single-scattering approximation (reviewed by Sayers and Bunker, 1988) implemented in a computer code written by G. George (SSRL). The general procedure for data reduction of EXAFS spectra was as follows (Teo,

[2] For several model compounds, both fluorescence and transmission spectra were collected. Data analysis showed no significant differences in numerical results using either model spectra (O'Day, 1992; O'Day *et al.*, 1994b).

1986; Brown *et al.*, 1988; Lytle, 1989; Sayers and Bunker, 1988): 1) Multiple scans were averaged and energy calibration checked by assigning the maximum of the K-edge absorption peak to k = 0 = 7725 eV. In a few spectra, sharp glitches due to monochromator flaws were removed by deletion of one or two points. 2) Background below the K-edge was estimated by a linear fit through the pre-edge region (≈7400–7700 eV), extrapolated through the EXAFS region, and subtracted from the spectrum. 3) Background absorption above the K-edge was determined by fitting a cubic spline with 3 or 4 points using Victoreen coefficients (Teo, 1986; Brown *et al.*, 1988) from 7725 eV to 8300–8400 eV. Spectra were normalized using tabulated McMaster coefficients (McMaster *et al.*, 1969), converted from photon energy E (eV) to k ($Å^{-1}$) (Eq. 4), and weighted by k^3 or k^2 to account for damping of the EXAFS oscillations at high k. 4) Normalized spectra were windowed with an unsmoothed Gaussian function over a range of k = 3.0–3.2 to 11–13 (depending on data quality) and Fourier-transformed from k-space to R (distance)-space to produce radial structure functions (RSFs). Radial structure functions are shown uncorrected for phase shift; thus, distances are ≈0.3–0.4 Å shorter than actual distances between the absorber and backscatterer atoms. Spurious peaks in the RSFs due to spectral noise and Fourier termination effects were identified by changes in peak position in R-space when the k-limits of the transform were changed (Lytle, 1989). 5) Filtered EXAFS spectra were obtained by individually back-Fourier transforming major peaks in the RSFs (smoothed Gaussian window = 0.1 Å) in order to isolate individual contributions to the EXAFS (Cramer and Hodgson, 1979; Sayers and Bunker, 1988).

Non-linear least-squares curve-fitting methods were used to fit reference phase-shift and amplitude functions to filtered unknown spectra. Empirical phase-shift and amplitude functions from dry, crystalline $Co(OH)_2$(s) were used for Co-O (R = 2.097 Å, N = 6) and Co-Co (R = 3.173 Å, N = 6) correlations. In the absence of suitable experimental model compound spectra, the *ab initio* theoretical EXAFS code FEFF v. 5 (Mustre de Leon *et al.*, 1991; Rehr *et al.*, 1991, 1992) was used to generate reference phase-shift and amplitude functions for Co-Al or Co-Si absorber-backscatterer pairs. Calculations with FEFF showed that multiple-scattering paths do not contribute significant amplitude to the EXAFS at path lengths <6 Å, but that linear multiple-scattering is important among Co atoms at ≈3 Å and 6 Å. Threshold energies (ΔE_0 = difference between E_0 for the reference and unknown spectra) for the theoretical Co functions from FEFF were calibrated on the experimental $Co(OH)_2$(s) spectrum. In the least-squares analysis, R, N, σ^2, and ΔE_0 for first-shell fits, and R, N, and σ^2 for >first-shell fits, were treated as adjustable parameters.[3] It is assumed that parameters in Eq. (3) not directly measured or calculated are the same in the unknown and the reference and thus cancel (Lytle, 1989; Brown *et al.*, 1988; Chisholm-Brause *et al.*, 1990a). It should be noted, however, that none of the adjusted parameters is entirely independent, and in particular, N and σ^2 are positively correlated to a high degree (Crozier et al., 1988). Relative errors for experimental and theoretical reference functions were estimated by analyzing a series of well-characterized model compounds with similar first-shell oxygen and greater-shell metal atom backscatterers as unknowns (O'Day, 1992). By this method, maximum errors for distance (R) and backscatterer number (N) are: Co-O, R ± 0.02 Å, N ± 25%; Co-Co, R ± 0.02 Å, N ± 20%; Co-Al or Si, R ± 0.02 Å, N ± 30%. Goodness-of-fit in the least-squares analysis of unknown spectra are given in the form of a reduced χ^2 parameter, ϵ^2, calculated by

$$\epsilon^2 = \frac{1}{\nu} \sum_{i=1}^{N} (\text{Data}_i - \text{Model}_i)^2 \qquad (5)$$

where ν is (N − p), N is the number of data points, p is the number of fit parameters, ($\text{Data}_i - \text{Model}_i$) is the difference between the experimental data and the model for each point i, and s_i^2 is the standard deviation of each point i (Report on the international workshops on standards and criteria in XAFS, 1991). The type of backscattering atoms assumed to surround a central Co atom is determined by trial and error. In most cases, phase-shift and amplitude functions for possible backscattering atoms are sufficiently characteristic that choice of the backscattering atom type(s) is obvious. After best fits are obtained for the filtered EXAFS, the sum of the calculated fits from all shells is compared to the normalized EXAFS spectrum with no Fourier filtering and, if necessary, minor adjustments to the fit are made. This procedure accounts for overlap in backscatterer phase-shift and amplitude functions and eliminates possible errors introduced by Fourier transform windowing.

XAS RESULTS

Edge structure

Figure 3 shows X-ray absorption spectra of the Co K-edge for representative sorption samples compared to spectra for an aqueous 12 mM $Co(NO_3)_2$ solution and two solid model compounds, $Co(OH)_2$(s) and $CoAl_2O_4$(s). In all sorption samples, the shape of the Co K-edge is similar to that of reference spectra in which Co is six-coordinated ($Co(NO_3)_2$(aq) and

[3] In practice, ΔE_0 has been found to depend on the absorber atom in most materials, and thus, it can be treated as an adjustable parameter in fits to the first coordination shell and then fixed in other fits (O'Day, 1992; O'Day *et al.*, 1994b).

https://doi.org/10.1346/CCMN.1994.0420312 Published online by Cambridge University Press

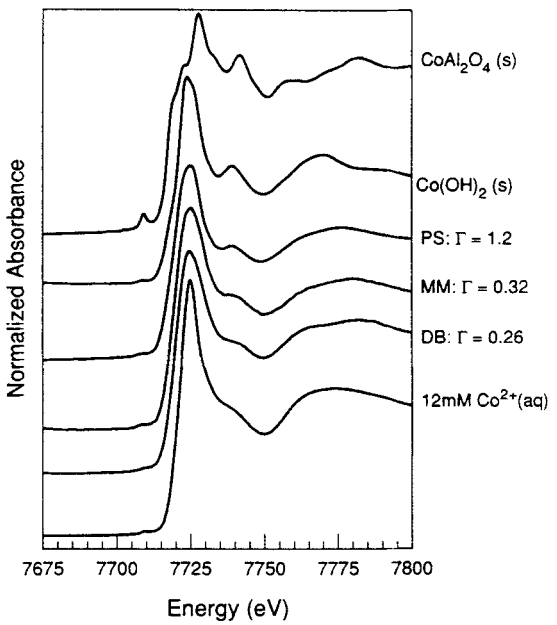

Figure 3. Normalized Co K-edge X-ray absorption spectra for aqueous 12 mM $Co(NO_3)_2$ solution, kaolinite sorption samples at surface sorption densities (Γ) = 0.26 (DB), 0.32 (MM), and 1.2 (PS) μmol m^{-2}, and $Co(OH)_2$(s) and $CoAl_2O_4$(s) model compounds. Note the pre-edge feature at ≈7709 eV indicative of 4-coordinated Co in the spectrum of $CoAl_2O_4$(s) that is very small in other spectra in which Co is 6-coordinated in a regular octahedral site.

$Co(OH)_2$(s)), but differs markedly from the spectrum of $CoAl_2O_4$(s) in which Co is four-coordinated. The latter spectrum contains a prominent pre-edge feature at ≈7709 eV that corresponds to a bound state 1s to 3d orbital electronic transition (Brown *et al.*, 1988; Chisholm-Brause *et al.*, 1990b). This transition is characteristic of tetrahedrally coordinated metal cations, but it is not allowed when the bonding environment around the metal cation has a center of inversion as in octahedral coordination (Calas and Petiau, 1983; Waychunas *et al.*, 1983). The small size of the pre-edge feature in the sorption samples, regardless of sorption density, indicates little distortion of the oxygen octahedron around Co. If oxidation of Co(II) to Co(III) occurred to a significant extent in the sorption samples, it would result in a detectable shift in the K-edge to higher energy by as much as 5 eV and in changes in the shape of the edge spectrum (Brown *et al.*, 1988). Based on these criteria, there is no evidence for oxidation in any of the sorption samples.

EXAFS results

Normalized EXAFS spectra for Co sorbed to Dry Branch (DB) kaolinite are shown in Figure 4a for samples with surface coverages from 0.26–2.6 μmol m^{-1}. At the lowest Co coverages, EXAFS spectra are similar in character to the spectrum of aqueous 12 mM

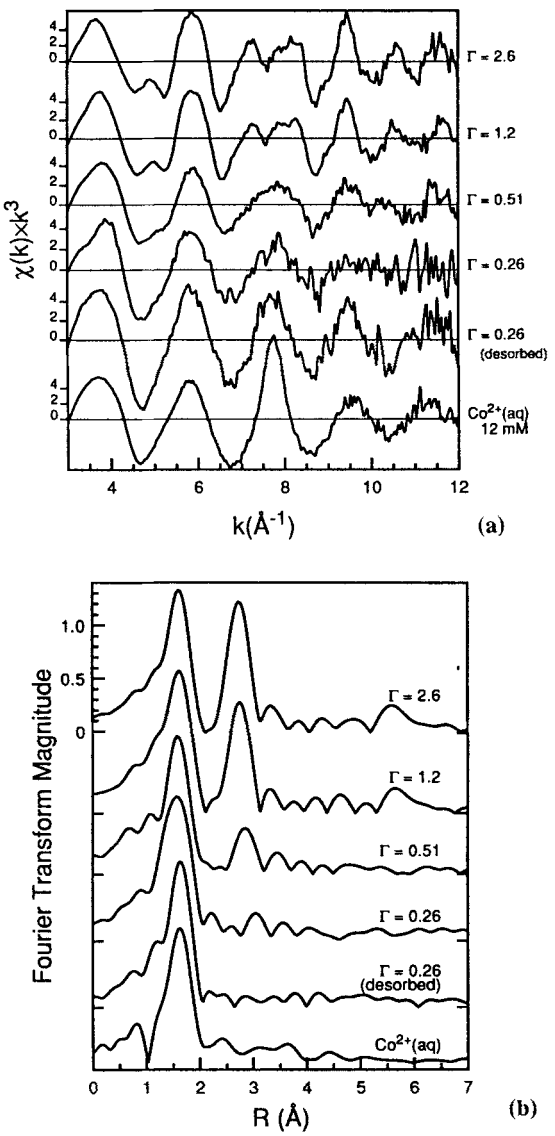

Figure 4. a) Normalized, background-subtracted EXAFS spectra weighted by k^3 of Co sorbed on DB kaolinite at surface sorption densities (Γ, μmol m^{-2}) shown compared to spectrum for aqueous 12 mM $Co(NO_3)_2$ solution. b) Radial structure functions (RSFs) produced by forward Fourier transforms of spectra shown in (a) (uncorrected for phase shift). Note the appearance of a peak at R ≈2.7 Å in Γ = 0.51 μmol m^{-2} spectrum, and the appearance of a peak at high R (≈5.8 Å) in the spectra for Γ = 1.2 and 2.6 μmol m^{-2}.

$Co(NO_3)_2$ solution in which the only backscattering atoms are 6 O at a distance of 2.10 Å (Table 3). With increased loading (Γ = 1.2 and 2.6 μmol m^{-2}), complicated "beat" patterns are evident in the EXAFS (Figure 4a) and indicate the presence of backscattering atoms beyond the first coordination shell. Fourier transforms of these spectra (Figure 4b) indicate changes in absorber-backscatterer correlations that change with

https://doi.org/10.1346/CCMN.1994.0420312 Published online by Cambridge University Press

Table 3. Distance (R), number of backscattering atoms (N), Debye-Waller factor (σ^2), difference in threshold energy (ΔE_o), and reduced statistical goodness-of-fit value (ϵ^2, given by Eq. 5) for sorption samples from non-linear least-squares fits of filtered EXAFS spectra.

Dry Branch kaolinite

Γ	Co-O					Co-Co			Co-Al/Si				
(10^{-6} mol m^{-2})	R(Å)	N	σ^2(Å^2)	ΔE_o(eV)	ϵ^2	R(Å)	N	σ^2(Å^2)	R(Å)	N	σ^2(Å^2)	ΔE_o(eV)	ϵ^2
2.6	2.08	6.8	0.0063	−2.6	0.08	3.11	3.5	0.0046	3.15	1.2	0.0056	3.0	0.13
1.2	2.08	6.9	0.0080	−0.4	0.06	3.12	2.1	0.0036	3.15	0.7	0.0044	1.2	0.05
0.51	2.07	6.2	0.0078	−1.3	0.12	3.13	0.7	0.0038	3.38	0.7	0.0043	1.0	0.01
0.26	2.08	7.2	0.0090	−1.0	0.15								
0.26, desorbed[1]	2.08	8.1	0.0047	−2.8	0.19								

Purvis School kaolinite

Γ	Co-O					Co-Co			Co-Al/Si				
(10^{-6} mol m^{-2})	R(Å)	N	σ^2(Å^2)	ΔE_o(eV)	ϵ^2	R(Å)	N	σ^2(Å^2)	R(Å)	N	σ^2(Å^2)	ΔE_o(eV)	ϵ^2
1.2	2.07	6.3	0.0059	−3.3	0.12	3.12	2.2	0.0035	3.14	1.4	0.0044	3.0	0.03
0.57	2.04	6.2	0.0120	−2.0		3.12	0.8	0.0031	2.72	0.9	0.0030	0.0	0.20[2]
									3.38	0.9	0.0065		
0.28	2.06	6.0	0.0081	−1.9					2.68	0.7	0.0062	0.0	0.29[2]
									3.39	1.2	0.0067		
0.21	2.04	6.9	0.0107	−2.3	0.30								

M&M kaolinite

Γ	Co-O				Co-Al/Si				
(10^{-6} mol m^{-2})	R(Å)	N	σ^2(Å^2)	ΔE_o(eV)	R(Å)	N	σ^2(Å^2)	ΔE_o(eV)	ϵ^2
0.32	2.09	6.1	0.0096	2.0	2.69	0.6	0.0040	0.7	0.21[2]
					3.43	1.5	0.0040		
0.30	2.05	6.6	0.0119	−1.7	2.68	0.7	0.0035	−1.0	0.34[2]
					3.40	1.1	0.0052		
0.20	2.06	5.9	0.0083	−0.1	2.67	0.8	0.0105	1.0	0.15[2]
					3.43	0.9	0.0060		

Reference compounds

	Co-O		Co-Co		
	R(Å)	N	R(Å)	N	Reference
$Co(OH)_2$(s)	2.097	6	3.173	6	Lotmar and Feitknecht (1936)
$Co(NO_3)_{2(aq)}$	2.108	6	—	—	Bol *et al.* (1970)

Empirical phase-shift and amplitude functions derived from the experimental spectrum of aged, crystalline $Co(OH)_2$(s) using R and N from XRD analysis (Lotmar and Feitknecht, 1936) were used as the reference functions for Co-O and Co-Co fits. Theoretical phase-shift and amplitude functions generated by FEFF v. 5 (Mustre de Leon *et al.*, 1991; Rehr *et al.*, 1991, 1992) from an atomic cluster model were used as the reference functions for Co-Al/Si fits. Difference in threshold energy (ΔE_o) was determined by treating E_o as an adjustable parameter in fits of the Co-O coordination shell; ΔE_o was fixed in fits of higher R shells.

[1] Co(II) desorbed to 14% uptake after equilibration for 24 h at 90% uptake.

[2] Reduced least-squares error (see Eq. 5) to EXAFS filtered over RSF peaks from ≈0.3–3.2 Å.

increasing surface coverage. In all spectra, least-squares fits of filtered EXAFS of the first RSF peak indicate ≈6 O atoms at 2.07–2.08 Å (Table 3).[4] At the lowest uptakes, no peaks above background are evident in the RSF other than the first peak (Figure 4b). In the RSF for Γ = 0.51 μmol m^{-2}, there is a small peak at ≈2.7 Å. In the RSF for 1.2 and 2.6 μmol m^{-2}, the location of this peak shifts to slightly lower R and increases in amplitude. Also note in these RSFs a peak above background at ≈5.8 Å (Figure 4b). Analyses of the peaks at 2.7 Å and 5.8 Å (discussed below) indicate that they are primarily a result of increasing numbers of Co neighbor atoms at a distance of ≈3.1 Å (corrected for phase shift) and the 5.8 Å peak results from multiple-scattering among Co atoms at both 3.1 Å and 6.2 Å.

To better understand the nature of the changes in Co bonding on kaolinite with increasing surface coverage suggested by the DB spectra, EXAFS spectra of DB kaolinite are compared to those of Co sorbed to Purvis School (PS) and M&M Mine (MM) kaolinite samples at the lowest surface coverages (Γ = 0.20–0.32 μmol m^{-2}; Figure 5a). Comparison of Fourier transforms of these spectra to those of DB at Γ = 0.26 μmol m^{-2} and aqueous Co^{2+} (Figure 5b) shows the presence of either one or two low amplitude peaks at distances greater than the first O peak. Filtered EXAFS spectra from R = 0.3–3.2 Å clearly indicate the presence of other backscattering atoms in addition to the first shell of six O atoms (Figure 6a). Non-linear least-squares fits of these spectra suggest the presence of Al and/or Si backscattering atoms (N = 0.6–1.5) at two distinct distances (R = 2.67–2.69 Å and 3.38–3.43 Å) in addition to O atoms at R = 2.04–2.09 Å (Figure 6b; Table 3). Backscattering from O atoms is too weak to detect beyond the ligating shell around Co (Teo, 1986). Therefore, the only other atoms present in sufficient concentration in the experimental system to possibly produce backscattering in the EXAFS are Ti, from TiO_2 particles present as a minor phase; Fe, present as a structural substituent as indicated by EPR studies (G. Calas, personal communication); or Co sorbed from solution. Because Fe and Co differ in atomic number by 1 (Z = 26 and 27, respectively), they cannot be distinguished from each other as backscatterers, although they should be distinguishable from Ti backscatterers (Z = 22). Least-squares fits assuming only these possible backscattering atoms—Co, Fe, or Ti—at distances consistent with bidentate bonding of Co and fixing the Co-O first-shell parameters produced poorer fits as indicated by higher ϵ^2 values (Figure 6c). If the dominant second-neighbor signal in the EXAFS was backscattering from Co, Fe, or Ti rather than Al or Si, the spectra should show higher backscattering amplitudes in a different k range (6–8 $Å^{-1}$) compared to Al or Si backscattering for which amplitudes decrease rapidly at k > 3–5 $Å^{-1}$ (Teo, 1986). Because an EXAFS spectrum is a composite of backscattering from all atoms, however, we cannot detect a small backscattering contribution from a low number of backscatterers.

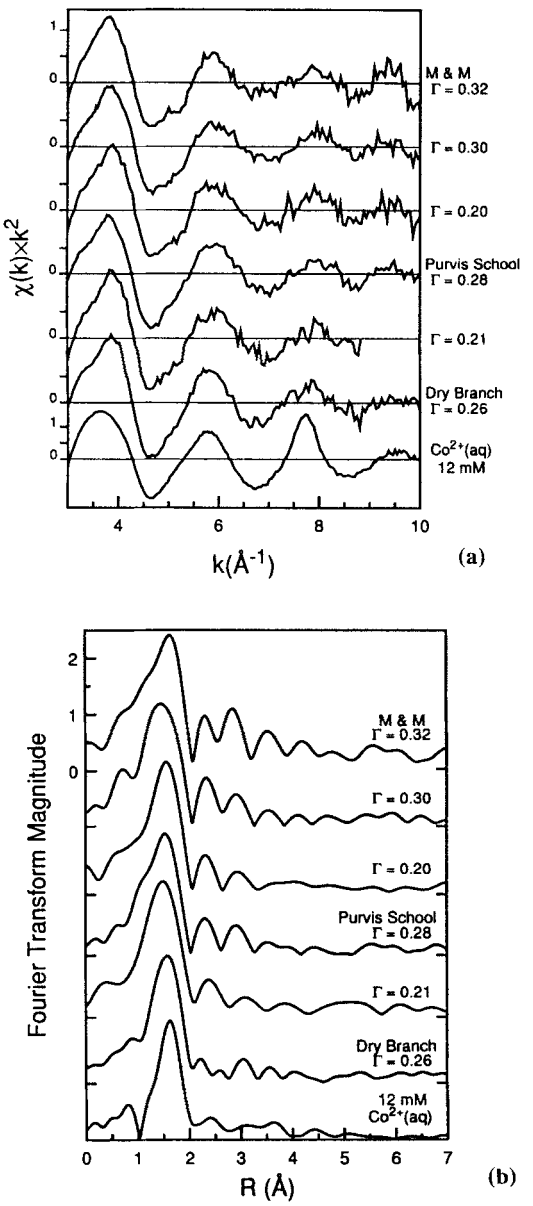

Figure 5. a) Normalized, background-subtracted EXAFS spectra weighted by k^2 of Co sorbed on MM and PS kaolinite at surface sorption densities (Γ, μmol m^{-2}) shown compared to spectra for aqueous 12 mM $Co(NO_3)_2$ solution and DB kaolinite from Figure 4. Some spectra were truncated at high k because low Co concentrations resulted in unacceptable noise levels. b) Radial structure functions (RSFs) produced by forward Fourier transforms of spectra shown in (a) (uncorrected for phase shift).

[4] Variation in the shape of the first peak in the RSF at low R results from small differences in the background fit and Fourier transform limits and does not affect numerical results.

https://doi.org/10.1346/CCMN.1994.0420312 Published online by Cambridge University Press

At the next highest surface coverages (0.51–0.57 μmol m^{-2}) on the three kaolinite samples (Figure 7), there are distinct differences among the EXAFS spectra for different kaolinites at similar Co sorption density. The RSF for PS at Γ = 0.57 μmol m^{-2} exhibits two peaks at R ≈ 2 Å to 3 Å, similar to the RSF for MM at Γ = 0.32 μmol m^{-2}, but having slightly higher amplitude for the peak at higher R (Figure 7b). For the PS sample, best fit of the filtered EXAFS from R = 0.3–3.2 Å requires the presence of a small number of Co atoms (N = 0.8) at 3.12 Å in addition to Al or Si atoms in order to reproduce the EXAFS oscillations (Figure 8). A sample with similar Co surface coverage on DB kaolinite (Γ = 0.51 μmol m^{-2}) shows only one peak in the RSF beyond the first-shell peak (Figure 7b). Best fit of the filtered EXAFS of the DB sample likewise requires both Al/Si and Co atoms at R = 3.38 Å and 3.13 Å, respectively, to model the EXAFS (Table 3). The spectrum lacks evidence, however, of backscattering from Al or Si atoms at R ≈ 2.7 Å as in the spectra for PS and MM kaolinite. The DB and PS samples at this surface coverage (Γ = 0.51 and 0.57 μmol m^{-2}, respectively) are the first spectra in which Co contributes to the EXAFS as a second-neighbor backscattering atom. The Co-Co distances derived from fits (R = 3.12–3.13 Å) require oxygen- or hydroxyl-bridging between Co atoms, implying the formation of some multinuclear complexes in addition to monomeric complexes.

When Co surface coverage is approximately doubled to Γ = 1.2 μmol m^{-2}, the RSFs for both DB and PS have a single peak between R ≈ 2–3 Å (Figure 7b). This peak represents contributions from both Al/Si and Co atoms, but because Co has a higher atomic weight than Al or Si, backscattering from Co dominates over that from Al or Si at similar distances. Best fits suggest that the number of Al or Si backscatterers is ≈1 as in the lower coverage samples, but these fits are less robust because of the strong backscattering from Co atoms (Figure 9). The number of backscattering Co atoms at R = 3.10–3.12 Å is ≈2 and there is no evidence for backscattering atoms at closer distances (Figure 7 and Table 3). As Co surface loading is increased to 2.6 μmol m^{-2} on DB kaolinite, the number of Co backscatterers increases, indicating an increase in the average number of Co atoms in the multinuclear complex, and distance remains constant within error (Table 3). The increase in second-neighbor Co atoms at 3.10–3.12 Å also corresponds to an increase in the amplitude of the peak at ≈5.8 Å in the RSFs of Γ = 1.2 and 2.6 μmol m^{-2} DB and PS samples (Figures 4b and 7b). Detailed analysis using FEFF (O'Day *et al.*, 1994a) shows that this peak is a result of linear multiple-scattering of total path length equal to 6.2 Å among a central Co atom, Co atoms at 3.1 Å, and a small contribution from Co atoms at 6.2 Å. At these surface coverages, the average numbers of second-neighbor Co atoms at 3.1 Å (N =

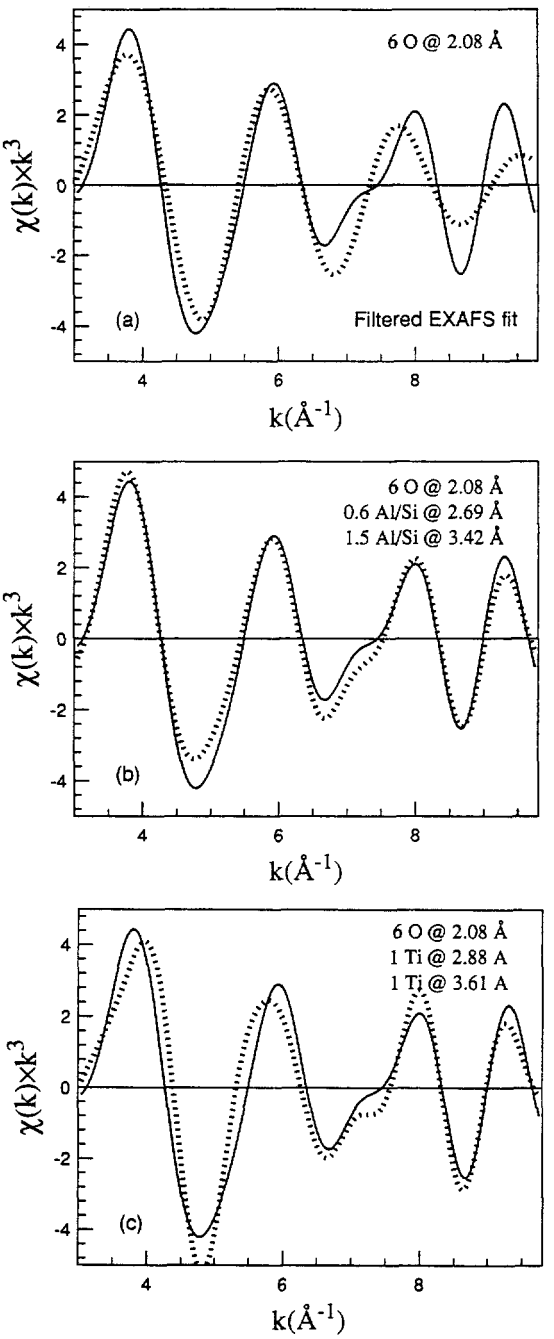

Figure 6. Filtered experimental EXAFS spectra (solid) and non-linear least-squares fits (dots) of MM kaolinite at Γ = 0.32 μmol m^{-2}: a) Fit assuming only O atoms as backscatterers. Reduced statistical goodness-of-fit value, ϵ^2 = 0.65. b) Fit assuming O atoms and Al or Si atoms as backscatterers at distances shown. ϵ^2 = 0.21. c) Fit assuming O atoms and Ti atoms as backscatterers at distances shown. ϵ^2 = 0.57.

https://doi.org/10.1346/CCMN.1994.0420312 Published online by Cambridge University Press

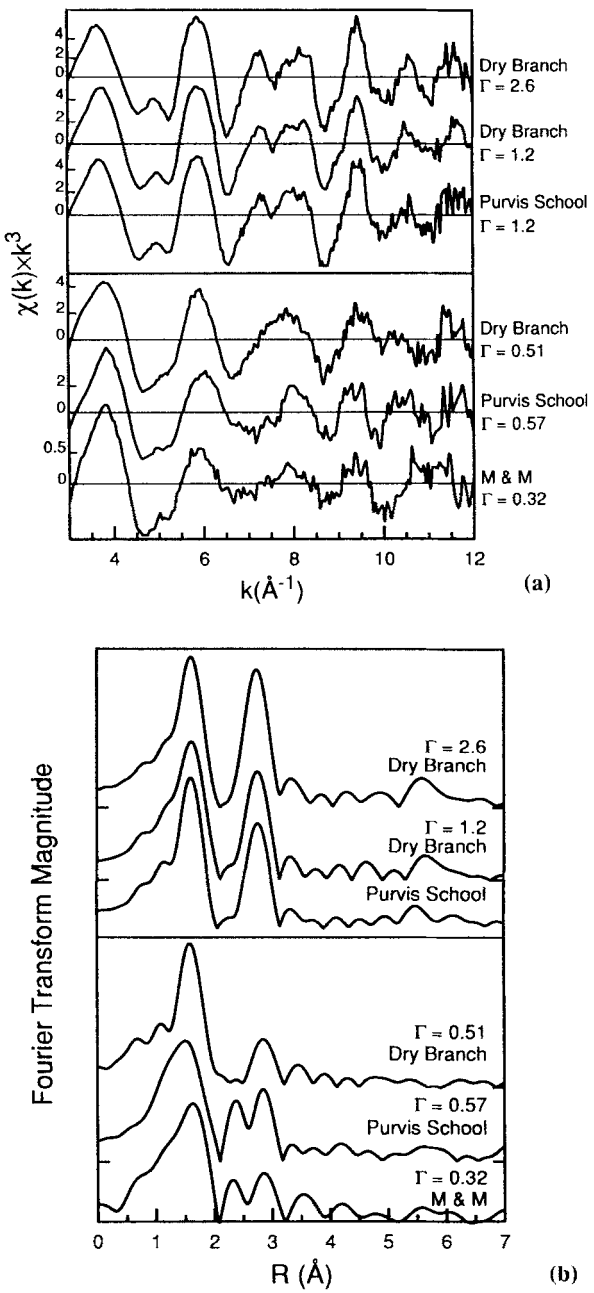

Figure 7. a) Normalized, background-subtracted EXAFS spectra weighted by k^3 of Co sorbed on DB, PS, and MM kaolinite at surface sorption densities (Γ, μmol m^{-2}) shown. All spectra were weighted by k^3 except for MM Γ = 0.32 μmol m^{-2} spectrum, which was weighted by k^2. Note the distinct differences in the EXAFS oscillations between the two sets of data. b) Radial structure functions (RSFs) produced by forward Fourier transforms of spectra shown in (a) (uncorrected for phase shift). Note that the RSF of DB Γ = 0.51 μmol m^{-2} lacks a peak at ≈2.4 Å compared to PS and MM samples at similar Γ. At the next highest surface coverages on PS and DB samples (Γ = 1.2 and 2.6 μmol m^{-2}), all spectra have similar RSF peaks that differ from peak positions at lower coverage.

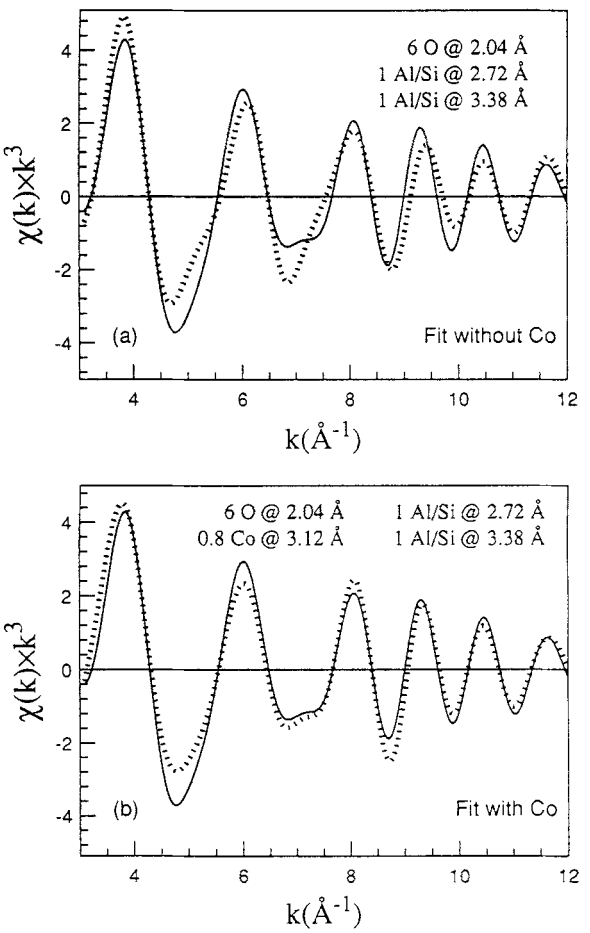

Figure 8. Filtered experimental EXAFS spectra (solid) and non-linear least-squares fits (dots) of PS kaolinite at Γ = 0.57 μmol m^{-2}: a) Fit assuming O and Al/Si atoms at two different distances ($\epsilon^2 = 0.31$); b) Fit assuming O, Al/Si, and Co atoms at distances shown ($\epsilon^2 = 0.20$).

2.1–3.5) and linear multiple-scattering paths are evidence for the presence of hydroxide-like Co clusters that are ordered on a local (≈3 Å) scale.

DISCUSSION

The EXAFS analysis of Co sorbed to kaolinite at low sorption densities can be summarized as follows:

1) At the lowest amounts of Co uptake (0.20–0.32 μmol m^{-2}), backscattering from O atoms at 2.04–2.09 Å and from a small number of Al or Si atoms (N = 0.6–1.5) at two distinct distances (2.68–2.72 Å and 3.38–3.43 Å) indicates that Co bonds to the kaolinite surface as octahedrally coordinated mononuclear complexes. Given octahedral coordination of Co, the closer Co-Al/Si distance (2.68–2.72 Å) is too long for tridentate bonding (<2.4 Å) and too short for a monodentate bond (>3.2 Å), but falls

https://doi.org/10.1346/CCMN.1994.0420312 Published online by Cambridge University Press

into the range of distances expected for bidentate bonding of Co octahedra to the surface.

2) The normalized EXAFS spectra and RSFs are not identical for all three kaolinites at similar surface loadings. At the lowest surface coverages, the DB RSFs lack a peak at R ≈ 2.7 Å, which is present in the other spectra. In the MM and PS samples, the amplitude of RSF peaks beyond the first-shell peak, attributed primarily to backscattering from Al or Si, is weak and variable. Backscattering predominantly from atoms present as impurities, either Ti or Fe, can be ruled out because their phase-shift and amplitude functions are distinctly different from Al or Si due to their higher atomic numbers.
3) At Γ = 0.51 and 0.57 μmol m^{-2} (DB and PS kaolinite), oxy- or hydroxy-bridged multinuclear complexes form in addition to mononuclear complexes (Co-Co distance = 3.10–3.13 Å, average N < 1). With increasing sorption densities (Γ = 1.2–2.6 μmol m^{-2}), the average number of Co second-neighbor atoms increases (N = 2.1–3.5), indicating multinuclear complexes with increasing numbers of Co atoms. The local structure of Co in the multinuclear complexes is similar to that of Co in $Co(OH)_2$(s), but Co-Co distances are shorter than those in $Co(OH)_2$(s) (3.10–3.12 Å *vs.* 3.17 Å). Locally ordered atomic clusters are indicated by contributions to the EXAFS from linear multiple-scattering paths.

Types of surface complexes on kaolinite

Interatomic distances of 2.67–2.72 Å and 3.38–3.43 Å for Co-Al/Si derived from EXAFS analysis indicate a direct bond between Co and oxygen atoms of the kaolinite surface. The low number of Al/Si backscatterers (N = 0.6–1.5) is evidence against significant diffusion of Co into the solid. The EXAFS results indicate formation of inner-sphere Co surface complexes, consistent with evidence from solution studies suggesting that one fraction of metal ions is sorbed specifically on kaolinite (Schindler *et al.*, 1987; Cowan *et al.*, 1992; Zachara *et al.*, 1994; O'Day, 1992). As discussed above, solution studies also indicate a fraction of sites that sorb ions weakly or nonspecifically and exhibit ion-exchange type behavior. Non-specific adsorption has been interpreted as evidence for the formation of outer-sphere complexes (Hayes and Leckie, 1987). Bonding of a hydrated Co ion to the surface by outer-sphere complexation would result in Co-Al/Si distances of >5 Å, which is beyond the range of typical single-scattering processes that produce EXAFS (Sayers *et al.*, 1971; Ashley and Doniach, 1975; Stern *et al.*, 1975; Teo, 1986). Thus, there is no direct evidence from EXAFS for the formation of outer-sphere complexes. The EXAFS spectra, however, could be comprised of backscattering contributions from a mixture of different concentrations of inner- and outer-sphere complexes

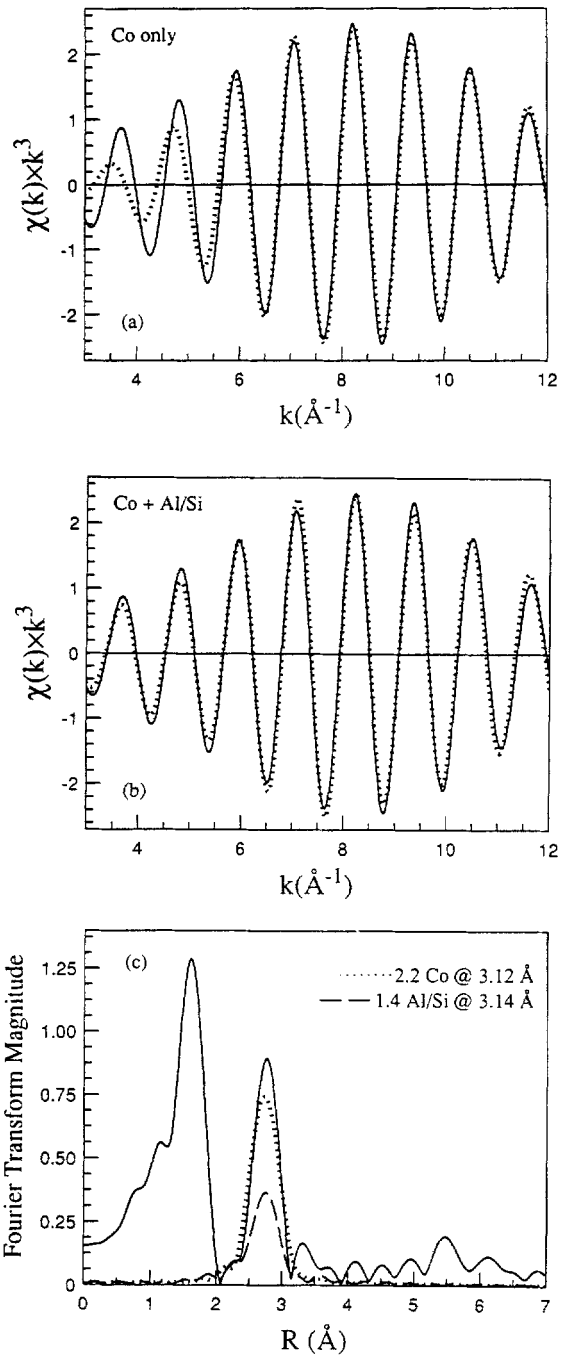

Figure 9. Filtered experimental EXAFS spectra (solid) and non-linear least-squares fits (dots) of second RSF peak of PS kaolinite at Γ = 1.2 μmol m^{-2}: a) Fit assuming Co atoms only (ϵ^2 = 0.10); b) Fit assuming Co and Al/Si atoms (ϵ^2 = 0.03); c) Deconvolution of fit shown in (b) into Co (dots) and Al/Si (dash) contributions to experimental RSF (solid).

https://doi.org/10.1346/CCMN.1994.0420312 Published online by Cambridge University Press

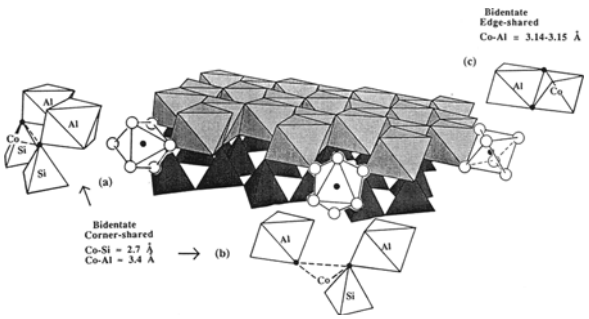

Figure 10. Possible modes of attachment of Co to the kaolinite surface. Corner-sharing between a Co octahedron and Al or Si polyhedra may occur on particle edges at two sites: a) Co may bond to two bridging Al-O-Si sites, or b) Co may bond to one bridging Al-O-Si and one Al-OH inner-hydroxyl site. Both of these atomic arrangements would give two Co–Al/Si distances (R ≈ 2.7 Å and 3.4 Å) consistent with EXAFS results at the lowest surface coverages. At slightly higher surface coverages, a single Co–Al/Si distance (R = 3.14–3.15 Å) from EXAFS analysis suggests that Co edge-shares with Al octahedra on either edges or (001) faces (c). Corner-sharing between Co and Al octahedra would result in a maximum distance of ≈4 Å, beyond the range of detection by EXAFS (d).

in which the first O coordination shell retains its regular octahedral coordination. In all sorption samples, a low degree of distortion around sorbed Co is indicated by EXAFS analysis of the ligating oxygen shell and by the small amplitude of pre-edge feature in the X-ray absorption edges, similar to that of Co in both $Co(NO_3)_2$(aq) and $Co(OH)_2$(s). The XAS results are in agreement with XPS studies of metal ions on clays that indicate a local electronic environment similar to aquo solution complexes (Koppelman and Dillard, 1975, 1977; Koppelman *et al.,* 1980; Dillard and Koppelman, 1982; Schenk *et al.,* 1983). In the lowest uptake samples, backscattering from Al/Si is weak and variable among the different kaolinite samples. This may be evidence for mixtures of inner- and outer-sphere complexes in different proportions, or may indicate some variability in sorption sites.

Analysis of surface sorption sites: Polyhedral approach

The interatomic distances and coordination environments around Co derived from EXAFS provide a basis for considering how Co may bond to the kaolinite surface as an inner-sphere complex. In the following discussion, a polyhedral approach is used (e.g., Manceau and Combes, 1988; Combes *et al.,* 1989, 1990) in which it is assumed that the ideal structure of kaolinite determined by XRD serves as the substrate (Figure 1) and that Co bonds to the surface as a regular, oxygen-coordinated octahedron with a minimum amount of distortion. The Co-Al/Si distances indicate bidentate bonding of adjacent O atoms in a Co octahedron of two general forms: 1) sharing of the edge of a Co octahedron with the corners of two adjacent polyhedra in the kaolinite structure ("corner-sharing"); or 2) sharing of the edge of a Co octahedron with the edge of a single polyhedron, either an Al octahedron or a Si tetrahedron, in kaolinite ("edge-sharing"). Thus, likely sites of attachment can be deduced by comparing O-O distances in Co octahedra with O-O distances in Si and Al polyhedra in the kaolinite structure, and then comparing the calculated Co-Al/Si distances at these sorption sites to those derived from EXAFS.

Bond distances in kaolinite calculated from XRD measurements (Young and Hewat, 1988; Bish and Von Dreele, 1989) show that O-O distances vary over a significant range because both Al octahedra and Si tetrahedra in kaolinite are distorted from ideal polyhedra. In general, however, edge O-O distances in Co octahedra (2.89–2.92 Å) derived from EXAFS Co-O distances (assuming a regular octahedron) are greater than edge O-O distances in Al octahedra (2.32–3.01 Å, mean = 2.76 Å) or Si tetrahedra (2.31–2.74 Å, mean = 2.54 Å) in kaolinite because of the larger size of the Co^{2+} ion. Edge-sharing between Co octahedra and Si tetrahedra is unlikely because of the large difference in O-O distances and strong cation-cation repulsion between Co^{2+} and Si^{4+} at such a close distance. In Al octahedra, O-O distances have a much wider range than those in Si tetrahedra, and some of the O-O distances in kaolinite overlap the average O-O distance in a Co octahedron. Therefore, edge-sharing is possible between a Co octahedron and a distorted Al octahedron. Edge-sharing of Co and Al octahedra, however, results in Co-Al distances on the order of 3.0–3.2 Å, which is significantly different from either of the Co-Al/Si distances (≈2.7 Å and ≈3.4 Å) derived from EXAFS analysis of the low uptake samples. Therefore, other sites of attachment for Co must be considered.

In kaolinite, there are two types of O-O distances that are slightly longer than O-O distances in Al octahedra and that overlap those observed for Co octahedra (2.89–2.92 Å) (Figure 10): 1) between two O atoms at adjacent Al-O-Si sites on (010) faces where O-O = 2.85–2.93 Å, mean = 2.89 Å; and 2) between O at an Al–O–Si site and O at an inner Al-OH site adjacent to an Al vacancy on (100) faces where O-OH = 2.76–3.14 Å, mean = 2.83 Å (see Figure 1). At the latter site, distances calculated from atom positions for O-OH are quite variable and indicate local distortion of polyhedra because of the Al vacancy. Based on simple electrostatic valence concepts, Al-OH and Al-O-Si sites exposed on particle edges have excess non-bonded electron density on oxygen atoms and are potential sites for cation binding. At both of these sites, bidentate attachment of Co would result in a geometry where the edge of a Co octahedron bridges the apicies of two Al octahedra and two Si tetrahedra (corner-sharing) rather than edge-sharing a polyhedron (Figure 10). The Co-

Al/Si distances derived from EXAFS are consistent with this configuration if the equatorial plane of the Co octahedron were near parallel to 1:1 layers or tilted slightly (5°–10°) toward the aluminol sheet. This geometry would give one (for the O-OH site) or two (for the O-O site) nearest Si neighbors at ≈2.7 Å and 2 Al neighbors at ≈3.4 Å. In contrast, if Co formed a monodentate bond to an edge or (001) face site, a wide range of distances to other Al or Si atoms is possible depending on the orientation of the Co octahedron relative to the surface. However, Co-Al/Si distances for a monodentate bond must all be greater than ≈3.2 Å and would not account for observed backscattering from atoms at ≈2.7 Å. Thus, from EXAFS analysis alone, we cannot discount monodentate complexes at low sorption density, but the bidentate geometry described above is one mode of bonding that is consistent with all of the distances derived from EXAFS.

One indication that different surface sites may sorb Co is the observation that the EXAFS spectra of DB samples lack a peak in the RFSs corresponding to the Co-Al/Si distance of ≈2.7 Å that is present in PS and MM samples up to $\Gamma = 0.57$ μmol m^{-2} (Figures 5b and 7b). In the DB sample in which Co was desorbed to $\Gamma = 0.26$ μmol m^{-2} (14% uptake) after equilibration at high pH (Table 1 and Figure 4), the absence of RSF peaks beyond the first-shell peak can be explained by a high proportion of Co^{2+}(aq) in the residual supernatant solution dominating the EXAFS signal. In the other DB sorption samples with ≥80% uptake from solution, it is not clear why backscattering from Al/Si at ≈2.7 Å is absent in the DB spectra at the lowest surface coverages. Possible explanations include: 1) more disorder or vacancies in the DB kaolinite structure, or a small amount of Co attachment to sites of impurities (TiO_2 particles or substituted Fe), such that there is phase cancellation from different backscatterers at different distances; 2) more outer-sphere complexation of Co, which would not be detected by EXAFS, than inner-sphere complexation at the lowest coverages on DB kaolinite than on the other two kaolinites; 3) a small amount of dissolution of kaolinite and resorption or reprecipitation of Al on the surface occupying or masking sorption sites.

The experimental data provide little support for any one of these explanations. Identification of a small number of second-neighbor atoms present as impurities is difficult because the EXAFS signal is an average of all backscattering atoms and is not sensitive to small numbers of backscatterers. There is no obvious correlation between chemical impurities in the bulk kaolinite (Table 1), XRD patterns, and the observed differences in EXAFS spectra. All three kaolinites have Al/Si ratios very close to ideal stoichiometry, suggesting little isomorphic substitution. The PS kaolinite has the highest concentration of impurities (Table 1), contains a small amount of smectite (from electron microscopy), and shows some loss of minor XRD reflections. Therefore, it might be expected to show differences in its EXAFS spectra rather than DB kaolinite. This is not supported, however, by comparison of PS EXAFS spectra to MM spectra at the lowest coverages which shows that they are very similar (Figure 5). These observations may indicate that, at low metal ion uptake, different surface sites may be energetically similar and compete for ion binding.

Transition from mononuclear to multinuclear complexes

For all sorption samples below $\Gamma = 0.32$ μmol m^{-2}, EXAFS analysis identifies the presence of only monomeric, inner-sphere Co complexes. At $\Gamma = 0.51$ (DB) and 0.57 (PS) μmol m^{-2}, multinuclear, inner-sphere Co surface complexes are indicated in addition to monomeric complexes by backscattering from Co second neighbors (Figures 7 and 8). At the first appearance of multinuclear complexes, the low average Co-Co coordination numbers ($N_{Co} < 1$) suggest mixtures of monomeric ($N_{Co} = 0$) and multinuclear complexes (e.g., dimers ($N_{Co} = 1$), trimers ($N_{Co} = 1$–2), or tetramers ($N_{Co} = 1.5$–2.5)) in which average N depends on whether the geometry of the complex is closest-packed or linear. Analysis of the EXAFS spectra shows that Co surface complexes retain their octahedral coordination and Co-Co distances of 3.10–3.13 Å indicate oxy- or hydroxy-bridged Co complexes (i.e., edge-shared Co octahedra). This geometry is similar to that of Co in $Co(OH)_2$(s) in which Co resides in closest-packed, edge-shared hydroxyl octahedra and Co-Co distances are 3.17 Å. These results imply that, at the earliest stage of formation, multinuclear complexes are hydroxide-like in structure but slightly contracted relative to $Co(OH)_2$(s).

At the next highest surface coverages on DB and PS kaolinites ($\Gamma = 1.2$ and 2.6 μmol m^{-2}), a single Co-Al/Si distance (3.14–3.15 Å) is observed, in contrast to the two different Co-Al/Si distances (≈2.7 Å and ≈3.4 Å) observed at lower coverage for MM and PS samples (Table 3). The Co-Al/Si distances at these surface coverages suggest edge-sharing between Co and Al octahedra. The change in Co-Al/Si distances between these two surface coverages indicates a change in the dominant inner-sphere sorption site from corner-sharing of a Co octahedron with two kaolinite polyhedra (described above) to edge-sharing of Co and Al octahedra (Figure 10). Because Al octahedra are smaller than Co octahedra (Al-Al distances in kaolinite are ≈3 Å), edge-sharing of Co and Al octahedra may explain the shorter Co-Co distances in the sorption samples relative to Co-Co distances in $Co(OH)_2$(s). Whether Co surface complexes bond to Al octahedra on kaolinite edges, (001) faces, or both cannot be determined because, given either of these geometries, backscattering from Si in

the siloxane sheet would be too distant to detect in the EXAFS.

Based on equilibrium stability constants for aqueous species (Baes and Mesmer, 1976), no multinuclear Co hydrolysis products are present in the solution phase in significant concentrations ($<10^{-12}$ M), either before or after equilibration with the solid, and Co is present almost exclusively as Co^{2+}(aq) (Figure 2b). The formation of multinuclear complexes occurs at very low surface sorption densities; for example, $\Gamma = 0.5$ μmol m^{-2} corresponds to an atomic density of 0.3 atoms nm^{-2} (averaged over the BET surface area of the sample). If closest-packing of CoO_6 polyhedra is assumed to constitute a monolayer of Co atoms, an atomic density of 0.3 atoms nm^{-2} corresponds to <5% of monolayer coverage. If sorption is assumed on pairs of Al-O-Si sites on edges only, this sorption density represents about 38% occupancy of this type of site (1.9 sites $nm^{-2} \div 2$) using the surface area of DB kaolinite. These observations suggest that surface crowding is not responsible for the formation of Co multinuclear species, and that they form on or near the kaolinite surface from solutions in which multinuclear complexes are not present in significant concentration. This implies that the mineral surface favors or promotes hydrolysis and multinuclear complex formation (discussed in O'Day *et al.*, 1994a).

SUMMARY AND CONCLUSIONS

Evidence from X-ray absorption spectroscopy, together with data from macroscopic studies of uptake of Co and other metal ions on kaolinite, can be used to describe the types of surface complexes present, their average molecular geometry, and their sites of attachment on the kaolinite surface. Uptake studies indicate two types of metal ion binding, "weak" and "strong," on kaolinite (Farrah *et al.*, 1980; Schindler *et al.*, 1987; O'Day, 1992; Cowan *et al.*, 1992; Zachara *et al.*, 1992); this implies the presence of at least two types of surface complexes and/or surface sites. Results from Co EXAFS analysis at low surface sorption density confirm the presence of octahedrally coordinated inner-sphere complexes that would account for "strong" or specific binding of metal cations. The presence of outer-sphere complexes that may account for "weak" or non-specific uptake behavior cannot be detected directly by EXAFS when inner-sphere complexes are dominant. However, differences in the EXAFS spectra among different kaolinites at the lowest Co loadings may indicate mixtures of inner- and outer-sphere complexes as suggested by uptake data, or perhaps a minor amount of uptake on sites of chemical impurities averaged into the EXAFS signal.

For Co inner-sphere complexes, distances to nearest neighbor Al/Si atoms at the lowest surface coverages suggest that the dominant mode of attachment of Co to the surface is bidentate, although monodentate sites of attachment with longer (>3.4 Å) Co-Al/Si distances cannot be ruled out entirely based on EXAFS analysis. Using a polyhedral approach to bonding, two possible edge sites are proposed for bidentate bonding of a Co octahedron that are consistent with the two different Co-Al/Si distances ($\approx$2.7 Å and $\approx$3.4 Å) derived from EXAFS: 1) corner-sharing with adjacent Al-O-Si sites, or 2) corner-sharing with one Al-O-Si site and one Al-OH inner hydroxyl site at an Al vacancy (Figure 10). From valence bonding rules, Al-OH and Al-O-Si sites exposed on particle edges have excess non-bonded electron density on oxygen atoms and, thus, are potential sites for cation binding. Previous macroscopic models of metal ion uptake on kaolinite, however, have not explicitly included the Al-O-Si site as a binding site. In models in which two sites of specific adsorption are included, either non-bridging Al-OH and Si-OH sites (Riese, 1982; Zachara *et al.*, 1988; Carroll-Webb and Walther, 1988; Carroll and Walther, 1990; Singh and Mattigod, 1992; Xie and Walther, 1992) or non-bridging and bridging Al-OH sites (Wieland and Stumm, 1992) are assumed. In addition, few models have considered explicitly bidentate bonding of the metal ion to the kaolinite surface as did Schindler *et al.* (1987). The structural information from EXAFS analysis should be used in sorption models to verify that the atomic structures derived from spectroscopy are consistent with macroscopic uptake behavior.

With increased surface loading, EXAFS analysis shows that mixtures of mononuclear and multinuclear inner-sphere complexes form on the kaolinite surface at low sorption densities (<5% coverage of the BET surface area) without formation of multinuclear species in solution. These complexes form as oxy- or hydroxy-bridged species similar in local structure, but not identical to, $Co(OH)_2$(s). This is in agreement with measurements of electronic structure from XPS. As the number of Co atoms in multinuclear complexes increases with increasing sorption density, a single Co-Al/Si distance (3.14–3.15 Å) indicative of edge-sharing between Co and Al octahedra is observed, in contrast to the two different Co-Al/Si distances ($\approx$2.7 Å and $\approx$3.4 Å) found at lower coverage. The EXAFS results indicate a contraction of metal-metal distances, perhaps as a consequence of edge-sharing between Co octahedra and smaller Al octahedra. These results suggest that the formation of multinuclear complexes is not simply the addition of Co atoms to an existing surface complex with no change in bonding. Rather, their formation is accompanied by a change in the geometry of the Co complex relative to backscattering atoms of the substrate. From the analysis of interatomic distances, we suggest a change from corner-sharing on particle edges to edge-sharing on either particle edges or (001) faces of the aluminol sheet. With increasing uptake, multinuclear complexes increase in size and

may serve as precursors to surface precipitates that form at higher pH and surface sorption densities.

ACKNOWLEDGMENTS

Kaolinite samples and their chemical analyses and XRD patterns were kindly provided by Howard May, U.S. Geological Survey, Boulder, Colorado. We thank the staffs of SSRL (supported by the Department of Energy and the National Institute of Health) and NSLS for help with our XAS experiments and the members of the Brown/Parks research group for assistance with data collection. Thanks to Cathy Chisholm-Brause, Graham George, Britt Hedman, Keith Hodgson, Bill Jackson, Farrel Lytle, and Glenn Waychunas for help with experimental design, computer hardware and software, and data collection, analysis, and interpretation at various stages of this study. We thank John Rehr and Steve Zabinsky, University of Washington, for advance access to FEFF v. 5 and their assistance with the application of their program to this study. Hillary Thompson provided helpful comments for improving the manuscript. Financial support for this study was provided by the National Science Foundation through grants EAR-8805440 and EAR-9105015.

REFERENCES

Ashley, C. A. and Doniach, S. (1975) Theory of extended X-ray absorption fine structure (EXAFS) in crystalline solids: *Phys. Rev.* **B11,** 1279–1288.

Baes Jr., C. F. and Mesmer, R. E. (1976) *The Hydrolysis of Cations:* John Wiley & Sons, New York, 489 pp.

Bancroft, G. M. and Hyland, M. M. (1990) Spectroscopic studies of adsorption/reduction reactions of aqueous metal complexes on sulphide surfaces: in *Mineral-Water Interface Geochemistry,* M. F. Hochella Jr. and A. F. White, eds., *Reviews in Mineralogy* **23,** Mineralogical Society of America, Washington, D.C., 511–558.

Bish, D. L. and Von Dreele, R. B. (1989) Rietveld refinement of non-hydrogen atomic positions in kaolinite: *Clays & Clay Minerals* **37,** 289–296.

Bleam, W. F. and McBride, M. B. (1985) Cluster formation *vs.* isolated-site adsorption. A study of Mn(II) and Mg(II) adsorption on boehmite and goethite: *J. Colloid Interface Sci.* **103,** 124–132.

Bol, W., Gerrits, G. J. A., and van Panthaleon van Eck, C. L. (1970) The hydration of divalent cations in aqueous solution. An X-ray investigation with isomorphous replacement: *J. Appl. Cryst.* **3,** 486–492.

Bolland, M. D. A., Posner, A. M., and Quirk, J. P. (1976) Surface charge in kaolinites in aqueous suspension: *Aust. J. Soil Res.* **14,** 197–216.

Bolland, M. D. A., Posner, A. M., and Quirk, J. P. (1980) pH-independent and pH-dependent surface charges on kaolinite: *Clays & Clay Minerals* **28,** 412–418.

Brown Jr., G. E. (1990) Spectroscopic studies of chemisorption reaction mechanisms at oxide-water interfaces: in *Mineral-Water Interface Geochemistry,* M. F. Hochella Jr. and A. F. White, eds., *Reviews in Mineralogy* **23,** Mineralogical Society of America, Washington, D.C., 309–363.

Brown Jr., G. E., Calas, G., Waychunas, G. A., and Petiau, J. (1988) X-ray absorption spectroscopy and its applications in mineralogy and geochemistry: in *Spectroscopic Methods in Mineralogy and Geology,* F. C. Hawthorne ed., *Reviews in Mineralogy* **18,** Mineralogical Society of America, Washington, D.C., 431–512.

Brown Jr., G. E. and Parks, G. A. (1989) Synchrotron-based x-ray absorption studies of cation environments in earth materials: *Reviews of Geophysics* **27,** 519–533.

Brown Jr., G. E., Parks, G. A., and Chisholm-Brause, C. J. (1989) *In-situ* x-ray absorption spectroscopic studies of ions at oxide-water interfaces: *Chimia* **43,** 248–256.

Calas, G. and Petiau, J. (1983) Coordination of iron in oxide glasses through high-resolution K-edge spectra: Information from the pre-edge: *Solid State Comm.* **48,** 625–629.

Carroll, S. A. and Walther, J. V. (1990) Temperature dependence of kaolinite dissolution rates. *Amer. J. Sci.* **290,** 797–810.

Carroll-Webb, S. A. and Walther, J. V. (1988) A surface complex reaction model for the pH-dependence of corundum and kaolinite dissolution rates: *Geochim. Cosmochim. Acta* **52,** 2609–2623.

Charlet, L. and Manceau, A. (1992) X-ray absorption spectroscopic study of the sorption of Cr(II) at the oxide-water interface. II. Adsorption, coprecipitation, and surface precipitation on hydrous ferric oxide: *J. Colloid Interface Sci.* **148,** 443–458.

Chisholm-Brause, C. J. (1991) Spectroscopic and equilibrium study of cobalt(II) sorption complexes at oxide/water interfaces: Doctoral thesis, Stanford University, Stanford, California, 118 pp.

Chisholm-Brause, C. J., Hayes, K. F., Roe, A. L., Brown Jr., G. E., Parks, G. A., and Leckie, J. O. (1990a) Spectroscopic investigation of Pb(II) complexes at the γ-Al_2O_3/water interface: *Geochim. Cosmochim. Acta* **54,** 1897–1909.

Chisholm-Brause, C. J., O'Day, P. A., Brown Jr., G. E., and Parks, G. A. (1990b) Evidence for multinuclear metal-ion complexes at solid/water interfaces from X-ray absorption spectroscopy: *Nature* **348,** 528–530.

Combes, J. M., Manceau, A., Calas, G., and Bottero, J. Y. (1989) Formation of ferric oxides from aqueous solutions: A polyhedral approach by X-ray absorption spectroscopy. I. Hydrolysis and formation of ferric gels: *Geochim. Cosmochim. Acta* **53,** 583–594.

Combes, J. M., Manceau, A., and Calas, G. (1990) Formation of ferric oxides from aqueous solutions: A polyhedral approach by X-ray absorption spectroscopy. II. Hematite formation from ferric gels: *Geochim. Cosmochim. Acta* **54,** 1083–1091.

Cowan, C. E., Zachara, J. M., Smith, S. C., and Resch, C. T. (1992) Individual sorbent contributions to cadmium sorption on ultisols of mixed mineralogy: *Soil Sci. Soc. Am. J.* **56,** 1084–1094.

Cramer, S. P. and Hodgson, K. O. (1979) X-ray absorption spectroscopy: A new structural method and its applications to bioinorganic chemistry: *Prog. Inorg. Chem.* **25,** 1–39.

Crozier, E. D., Rehr, J. J., and Ingalls, R. (1988) Amorphous and liquid systems: in *X-ray Absorption: Principles, Applications, Techniques of EXAFS, SEXAFS, and XANES,* D. C. Koningsberger and R. Prins, eds., *Chemical Analysis* **92,** John Wiley & Sons, New York, 373–442.

Davis, J. A. and Hayes, K. F., eds. (1986) *Geochemical Processes at Mineral Surfaces, ACS Symposium Series* **323,** 683 pp.

Davis, J. A. and Kent, D. B. (1990) Surface complexation modeling in aqueous geochemistry: in *Mineral-Water Interface Geochemistry,* M. F Hochella Jr. and A. F. White, eds., *Reviews in Mineralogy* **23,** Mineralogical Society of America, Washington, D.C., 177–260.

Davison, N., McWhinnie, W. R., and Hooper, A. (1991) X-ray photoelectron spectroscopy study of cobalt(II) and

nickel(II) sorbed on hectorite and montmorillonite: *Clays & Clay Minerals* **39,** 22–27.

Dent, A. J., Ramsay, J. D. F., and Swanton, W. (1992) An EXAFS study of uranyl ion in solution and sorbed onto silica and montmorillonite clay colloids: *J. Colloid Interface Sci.* **150,** 45–60.

Dillard, J. G. and Koppelman, M. H. (1982) X-ray photoelectron spectroscopic (XPS) surface characterization of cobalt on the surface of kaolinite: *J. Colloid Interface Sci.* **87,** 46–55.

Dzombak, D. A. and Morel, F. M. M. (1990) *Surface Complexation Modeling: Hydrous Ferric Oxide:* John Wiley & Sons, New York, 393 pp.

Farley, K. J., Dzombak, D. A., and Morel, F. M. M. (1985) A surface precipitation model for the sorption of cations on metal oxides: *J. Colloid Interface Sci.* **106,** 226–242.

Farrah, H., Hatton, D., and Pickering, W. F. (1980) The affinity of metal ions for clay surfaces: *Chem. Geology* **28,** 55–56.

Feitknecht, W. and Schindler, P. (1963) Solubility constants of metal oxides, metal hydroxides and metal hydroxide salts in aqueous solution: *Pure Applied Chem.* **6,** 130–199.

Ferris, A. P. and Jepson, W. B. (1975) The exchange capacities of kaolinite and the preparation of homoionic clays: *J. Colloid Interface Sci.* **51,** 245–259.

Follet, E. A. C. (1965) The retention of amorphous, colloidal "ferric hydroxide" by kaolinites: *J. Soil Sci.* **16,** 334–341.

Fordham, A. W. (1973) The location of iron-55, strontium-85, and iodide-125 sorbed by kaolinite and dickite particles: *Clays & Clay Minerals* **21,** 175–184.

Gayer, K. H. and Garrett, A. B. (1950) The solubility of cobalt hydroxide, $Co(OH)_2$, in solutions of hydrochloric acid and sodium hydroxide at 25°C: *J. Amer. Chem. Soc.* **72,** 3921–3923.

Giese Jr., R. F. (1988) Kaolin minerals: Structures and stabilities: in *Hydrous Phyllosilicates,* S. W. Bailey, ed., *Reviews in Mineralogy* **19,** Mineralogical Society of America, Washington, D.C., 29–66.

Grim, R. E. (1968) *Clay Mineralogy:* McGraw-Hill, New York, 596 pp.

Hahn, J. E. and Hodgson, K. O. (1983) Polarized x-ray absorption spectroscopy: in *Inorganic Chemistry: Toward the 21st Century,* M. H. Chisholm, ed., *ACS Symposium Series* **211,** Washington, D.C., 432–444.

Hayes, K. F. and Leckie, J. O. (1987) Modeling ionic strength effects on cation adsorption at hydrous oxide/solution interfaces: *J. Colloid Interface Sci.* **115,** 564–572.

Hayes, K. F., Roe, A. L., Brown Jr., G. E., Hodgson, K. O., Leckie, J. O., and Parks, G. A. (1987) *In situ* X-ray absorption study of surface complexes at oxide/water interfaces: Selenium oxyanions on α-FeOOH: *Science* **238,** 783–786.

Heald, S. M. and Stern, E. A. (1977) Anisotropic X-ray absorption in layered compounds: *Phys. Rev.* **B16,** 5549–5559.

Hochella Jr., M. F. and White, A. F., eds. (1990) *Mineral-Water Interface Geochemistry, Reviews in Mineralogy* **23,** Mineralogical Society of America, Washington, D.C., 603 pp.

Jackson, M. L. (1975) *Soil Chemical Analysis—Advanced Course,* 2nd ed., published by the author, Department of Soil Science, University of Wisconsin, Madison, Wisconsin, 894 pp.

Jepson, W. B. and Rowse, J. B. (1975) The composition of kaolinite—an electron microscope microprobe study: *Clays & Clay Minerals* **28,** 310–317.

Koningsberger, D. C. and Prins, R., eds. (1988) *X-ray Absorption: Principles, Applications, Techniques of EXAFS, SEXAFS, and XANES, Chemical Analysis* **92,** John Wiley & Sons, New York, 673 pp.

Koppelman, M. H. and Dillard, J. G. (1975) An ESCA study of sorbed metal ions on clay minerals: in *Marine Chemistry in the Coastal Environment,* T. M. Church, ed., *ACS Symposium Series* **18,** Washington, D.C., 186–201.

Koppelman, M. H. and Dillard, J. G. (1977) A study of the adsorption of Ni(II) and Cu(II) by clay minerals: *Clays & Clay Minerals* **25,** 457–462.

Koppelman, M. H., Emerson, A. B., and Dillard, J. G. (1980) Adsorbed Cr(III) on chlorite, illite, and kaolinite: An X-ray photoelectron spectroscopic study: *Clays & Clay Minerals* **28,** 119–124.

Lee, S. Y., Jackson, M. L., and Brown, J. L. (1975) Micaceous occlusions in kaolinite observed by ultramicrotomy and high resolution electron microscopy: *Clays & Clay Minerals* **23,** 125–129.

Lim, C. H., Jackson, M. L., Koons, R. D., and Helmke, P. A. (1980) Kaolins: Sources of differences in cation-exchange capacities and cesium retention: *Clays & Clay Minerals* **28,** 223–229.

Lotmar, W. and Feitknecht, W. (1936) Uber anderungen der ionenabstande in hydroxyd-schichtengittern: *Z. Krist.* **A93,** 368–378.

Lytle, F. W. (1989) Experimental X-ray absorption spectroscopy: in *Applications of Synchrotron Radiation,* H. Winick et al., eds., Gordon and Breach Science Publ., 135–223.

Lytle, F. W., Sandstrom, D. R., Marques, E. C., Wong, J., Spiro, C. L., Huffman, G. P., and Huggins, F. E. (1984) Measurement of soft x-ray absorption spectra with a fluorescence ion chamber detector: *Nucl. Instr. and Meth.* **226,** 542–548.

Manceau, A., Bonnin, D., Kaiser, P., and Fretigny, C. (1988) Polarized EXAFS of biotite and chlorite: *Phys. Chem. Minerals* **16,** 180–185.

Manceau, A. and Charlet, L. (1992) X-ray absorption spectroscopic study of the sorption of Cr(II) at the oxide-water interface. I. Molecular mechanism of Cr(III) oxidation on Mn oxides: *J. Colloid Interface Sci.* **148,** 425–442.

Manceau, A., Charlet, L., Boisset, M. C., Didier, B., and Spadini, L. (1992) Sorption and speciation of heavy metals on hydrous Fe and Mn oxides. From microscopic to macroscopic: *Applied Clay Sci.* **7,** 201–223.

Manceau, A. and Combes, J. M. (1988) Structure of Mn and Fe oxides and oxyhydroxides: A topological approach by EXAFS: *Phys. Chem. Minerals* **15,** 283–295.

May, H. M., Kinniburgh, D. G., Helmke, P. A., and Jackson, M. L. (1986) Aqueous dissolution, solubilities and thermodynamic stabilities of common aluminosilicate clay minerals: Kaolinite and smectites: *Geochim. Cosmochim. Acta* **50,** 1667–1677.

McBride, M. B. (1976) Origin and position of exchange sites in kaolinite: An ESR study: *Clays & Clay Minerals* **24,** 88–92.

McBride, M. B. (1978) Copper(II) interactions with kaolinite: Factors controlling adsorption. *Clays & Clay Minerals* **26,** 101–106.

McBride, M. B., Fraser, A. R., and McHardy, W. J. (1984) Cu^{2+} interaction with microcrystalline gibbsite. Evidence for oriented chemisorbed copper ions: *Clays & Clay Minerals* **32,** 12–18.

McMaster, W. H., Del Grande, N. K., Mallett, J. H., and Hubbell, J. H. (1969) Compilation of x-ray cross sections III: U.S. Atom. Energ. Comm. **UCRL-50174.**

Motschi, H. (1984) Correlation of EPR parameters with thermodynamic stability constants for copper(II) complexes. Copper(II)-EPR as a probe for the surface complexation at the oxide/water interface: *Colloids Surf.* **9,** 333–347.

Motschi, H. (1987) Aspects of the molecular structure in surface complexes; spectroscopic investigations: in *Aquatic Surface Chemistry,* W. Stumm, ed., Wiley-Interscience, New York, 111–125.

Mustre de Leon, J., Rehr, J. J., and Zabinsky, S. I. (1991)

Ab initio curved-waved x-ray-absorption fine structure: *Phys. Rev.* **B44,** 4146–4156.

O'Day, P. A. (1992) Structure, bonding, and site preference of cobalt(II) sorption complexes on kaolinite and quartz from solution and spectroscopic studies: Doctoral thesis, Stanford University, Stanford, California, 208 pp.

O'Day, P. A., Brown Jr., G. E., and Parks, G. A. (1991) EXAFS study of aqueous Co(II) sorption complexes on kaolinite and quartz surfaces: in *X-ray Absorption Fine Structure,* S. S. Hasnain, ed., Ellis Horwood Ltd., London, 260–262.

O'Day, P. A., Brown Jr., G. E., and Parks, G. A. (1994a) X-ray absorption spectroscopy of cobalt(II) multinuclear surface complexes and surface precipitates on kaolinite: *J. Colloid Interface Sci.,* in press.

O'Day, P. A., Rehr, J. J., Zabinsky, S. I., and Brown Jr., G. E. (1994b) Extended X-ray absorption fine structure (EXAFS) analysis of disorder and multiple-scattering in complex crystalline solids: *J. Amer. Chem. Soc.,* in press.

Parfitt, R. L. (1978) Anion adsorption by soils and soil materials: *Adv. Agron.* **30,** 1–50.

Rehr, J. J. and Albers, R. C. (1990) Scattering-matrix formulation of curved-wave multiple-scattering theory: Application to X-ray-absorption fine structure: *Phys. Rev.* **B41,** 8139–8149.

Rehr, J. J., Albers, R. C., and Zabinsky, S. I. (1992) High-order multiple-scattering calculations of X-ray-absorption fine structure: *Phys. Rev. Lett.* **69,** 3937–3400.

Rehr, J. J., Mustre de Leon, J., Zabinsky, S. I., and Albers, R. C. (1991) Theoretical X-ray absorption fine structure standards: *J. Amer. Chem. Soc.* **113,** 5135–5140.

Report on the international workshops on standards and criteria in XAFS (1991): in *X-ray Absorption Fine Structure,* S. S. Hasnain, ed., Ellis Horwood Ltd., London, 751–770.

Riese, A. C. (1982) Adsorption of radium and thorium onto quartz and kaolinite: A comparison of solution/surface equilibria models: Doctoral thesis, Colorado School of Mines, Golden, Colorado, 210 pp.

Roe, A. L., Hayes, K. F., Chisholm-Brause, C. J., Brown Jr., G. E., Parks, G. A., and Leckie, J. O. (1991) X-ray absorption study of lead complexes at α-FeOOH/water interfaces: *Langmuir* **7,** 367–373.

Sayers, D. E. and Bunker, B. A. (1988) Data analysis: in *X-ray Absorption: Principles, Applications, Techniques of EXAFS, SEXAFS, and XANES,* D. C. Koningsberger and R. Prins, eds., *Chemical Analysis* **92,** John Wiley & Sons, New York, 211–253.

Sayers, D. E., Stern, E. A., and Lytle, F. W. (1971) New technique for investigating noncrystalline structures Fourier analysis of the Extended X-ray-Absorption Fine Structure: *Phys. Rev. Lett.* **27,** 1204–1207.

Schenk, C. V., Dillard, J. G., and Murray, J. W. (1983) Surface analysis and the adsorption of Co(II) on goethite: *J. Colloid Interface Sci.* **95,** 398–409.

Schindler, P. W., Liechti, P., and Westall, J. C. (1987) Adsorption of copper, cadmium, and lead from aqueous solution to the kaolinite/water interface: *Neth. J. Agri. Sci.* **35,** 219–230.

Schindler, P. W. and Stumm, W. (1987) The surface chemistry of oxides, hydroxides, and oxide minerals: in *Aquatic Surface Chemistry,* W. Stumm, ed., Wiley-Interscience, New York, 83–110.

Schofield, R. K. and Samson, H. R. (1954) Flocculation of kaolinite due to the attraction of oppositely charged crystal faces: *Faraday Soc. Diss.* **18,** 135–145.

Singh, S. P. N. and Mattigod, S. V. (1992) Modeling boron adsorption on kaolinite: *Clays & Clay Minerals* **40,** 192–205.

Sposito, G. (1984) *The Surface Chemistry of Soils:* Oxford University Press, New York, 234 pp.

Sposito, G. (1989) *The Chemistry of Soils:* Oxford University Press, New York, 277 pp.

Stern, E. A. (1988) Theory of EXAFS: in *X-ray Absorption: Principles, Applications, Techniques of EXAFS, SEXAFS, and XANES,* D. C. Koningsberger and R. Prins, eds., *Chemical Analysis* **92,** John Wiley & Sons, New York, 3–51.

Stern, E. A., Sayers, D. E., and Lytle, F. W. (1975) Extended X-ray absorption fine structure technique. III. Determination of physical parameters: *Phys. Rev.* **B11,** 4836–4846.

Stumm, W., ed. (1987) *Aquatic Surface Chemistry:* Wiley-Interscience, New York, 520 pp.

Stumm, W. (1992) *Chemistry of the Solid-Water Interface:* Wiley-Interscience, New York, 428 pp.

Talibudeen, O. (1981) Cation exchange in soils: in *The Chemistry of Soil Processes,* D. J. Greenland and M. H. B. Hayes, eds., John Wiley & Sons, New York, 115–177.

Talibudeen, O. and Goulding, K. W. T. (1983) Apparent charge heterogeneity in kaolins in relation to their 2:1 phyllosilicate content: *Clays & Clay Minerals* **31,** 137–142.

Teo, B.-K. (1986) *EXAFS: Basic Principles and Data Analysis. Inorganic Chemistry Concepts* **9,** Springer-Verlag, Berlin, 349 pp.

Teo, B.-K. and Joy, D. C., eds. (1981) *EXAFS Spectroscopy,* Plenum Press, New York, 275 pp.

Tewari, P. H., Campbell, A. B., and Lee, W. (1972) Adsorption of Co^{2+} by oxides from aqueous solution: *Can. J. Chem.* **50,** 1642–1648.

Tewari, P. H. and Lee, W. (1975) Adsorption of Co(II) at the oxide-water interface. *J. Colloid Interface Sci.* **52,** 77–88.

Tewari, P. H. and McIntyre, N. S. (1975) Characterization of adsorbed Co(II) at the oxide-water interface: *AICHE Symposium Series* **71**(150), 134–137.

van Olphen, H. (1977) *An Introduction to Clay Colloid Chemistry,* 2nd ed.: Wiley-Interscience, New York, 301 pp.

Waychunas, G. A. and Brown Jr., G. E. (1990) Polarized X-ray absorption spectroscopy of metal ions in minerals: Identification of near-edge electronic transitions and scattering resonances and application to site geometry determinations: *Phys. Chem. Minerals* **17,** 420–430.

Waychunas, G. A., Brown Jr., G. E., and Apted, M. A. (1983) X-ray K-edge absorption spectra of Fe minerals and model compounds: Near-edge structure: *Phys. Chem. Minerals* **9,** 212–215.

Wieland, E. and Stumm, W. (1992) Dissolution kinetics of kaolinite in acidic aqueous solutions at 25°C: *Geochim. Cosmochim. Acta* **56,** 3339–3355.

Winick, H. and Doniach, S., eds. (1980) *Synchrotron Radiation Research:* Plenum Press, New York, 680 pp.

Xie, Z. and Walther, J. V. (1992) Incongruent dissolution and surface area of kaolinite: *Geochim. Cosmochim. Acta* **56,** 3357–3363.

Young, R. A. and Hewat, A. W. (1988) Verification of the triclinic crystal structure of kaolinite: *Clays & Clay Minerals* **36,** 225–232.

Zachara, J. M., Cowan, C. E., Schmidt, R. L., and Ainsworth, C. C. (1988) Chromate adsorption by kaolinite: *Clays & Clay Minerals* **36,** 317–326.

Zachara, J. M., Resch, C. T., and Smith, S. C. (1994) Influence of humic substances on Co^{2+} sorption by a subsurface mineral separate and its mineralogical components: *Geochim. Cosmochim. Acta* **58,** 553–566.

(Received 29 March 1993; accepted 12 November 1993; Ms. 2358)